PART2

地球温暖化による台風の変化のメカニズム

I. なぜ地球温暖化により台風の数が減るのか

II. 台風の発生・発達のメカニズム

III. 最大可能強度（MPI）理論

IV. 発生ポテンシャル（GPI）

IPCC AR5 の結論

地球が温暖化すると

I. 台風全体の数が減る。

II. 強い台風の数が増える。

III. 台風の強度が強くなる。

IV. 台風の降水強度が強くなる。

I. なぜ地球温暖化により台風の数が減るのか

(1) Two hypotheses

1. Upward Mass Flux Hypothesis (Sugi)

2. Saturation Deficit Hypothesis (Emanuel)

Knutson et al. 2010, Nature GS :

Among the proposed mechanisms for the decrease in global tropical cyclone frequency is a weakening of the tropical circulation associated with a decrease in the upward mass flux accompanying deep convection, or an increase in the saturation deficit of the middle troposphere.

IPCC-AR5 (2013) Chapter 14 :

The decrease in storm frequency is apparently related to a projected decrease of upward deep convective mass flux and increase in the saturation deficit of the middle troposphere in the tropics associated with global warming (Bengtsson et al., 2007; Emanuel et al., 2008, 2012; Zhao et al., 2009; Held and Zhao, 2011; Murakami et al., 2012; Sugi et al., 2012; Sugi and Yoshimura, 2012).

Sugi et al. (2002) JMSJ

Influence of the Global Warming on Tropical Cyclone Climatology: An Experiment with the JMA Global Model

Masato SUGI, Akira NODA

Meteorological Research Institute, Tsukuba, Japan

and

Nobuo SATO

Japan Meteorological Agency, Tokyo, Japan

On the other hand, for the decrease in the global total number of tropical cyclones on doubling CO2, a weakening of tropical circulation associated with the stabilization of the atmosphere (the increase in dry static stability), seems to be responsible. It is found that the rate of increase in the tropical precipitation due to the global warming is much less than the rate of increase in the atmospheric moisture. With this little increase in precipitation (convective heating), a considerable increase in the dry static stability of the atmosphere leads to a weakening of the tropical circulation.

Sugi et al. 2002, JMSJ

Weakening of Tropical Circulation ⇒ Reduction of TC frequency

The wakening of tropical circulation due to global warming may be understood by energy balance of the tropical atmosphere. The approximate energy equation in the tropics may be expressed as,

$$\omega \frac{\partial \theta}{\partial p} \approx \frac{\theta}{T} \frac{Q}{C_p}, \tag{1}$$

(Holton 1979; Kuntson and Manabe 1995). Here we consider a schematic tropical circulation as shown in Fig. 13. Then, the energy balance in the upward motion region and downward motion region at 500 hPa may be written as,

$$M_u \left| \frac{\partial \theta}{\partial p} \right| \approx \frac{\theta}{T} \frac{1}{C_p} (Q_c - Q_R) A_u, \tag{2}$$

$$M_d \left| \frac{\partial \theta}{\partial p} \right| \approx \frac{\theta}{T} \frac{1}{C_p} Q_R A_d, \tag{3}$$

where $M_u(M_d)$ and $A_u(A_d)$ are the mass flux,

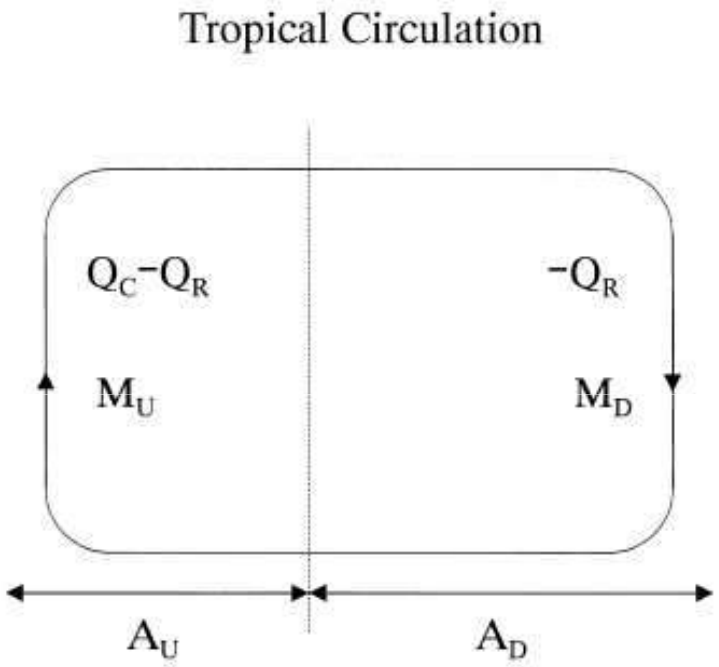

Fig. 13. A schematic diagram showing the energy balance of tropical circulation.

$$MS = Q \qquad \frac{\Delta M}{M} = \frac{\Delta Q}{Q} - \frac{\Delta S}{S} < 0$$

Weakening of Upward Velocity in CMIP3 Models

Vecchi and Soden (2007) JCLI

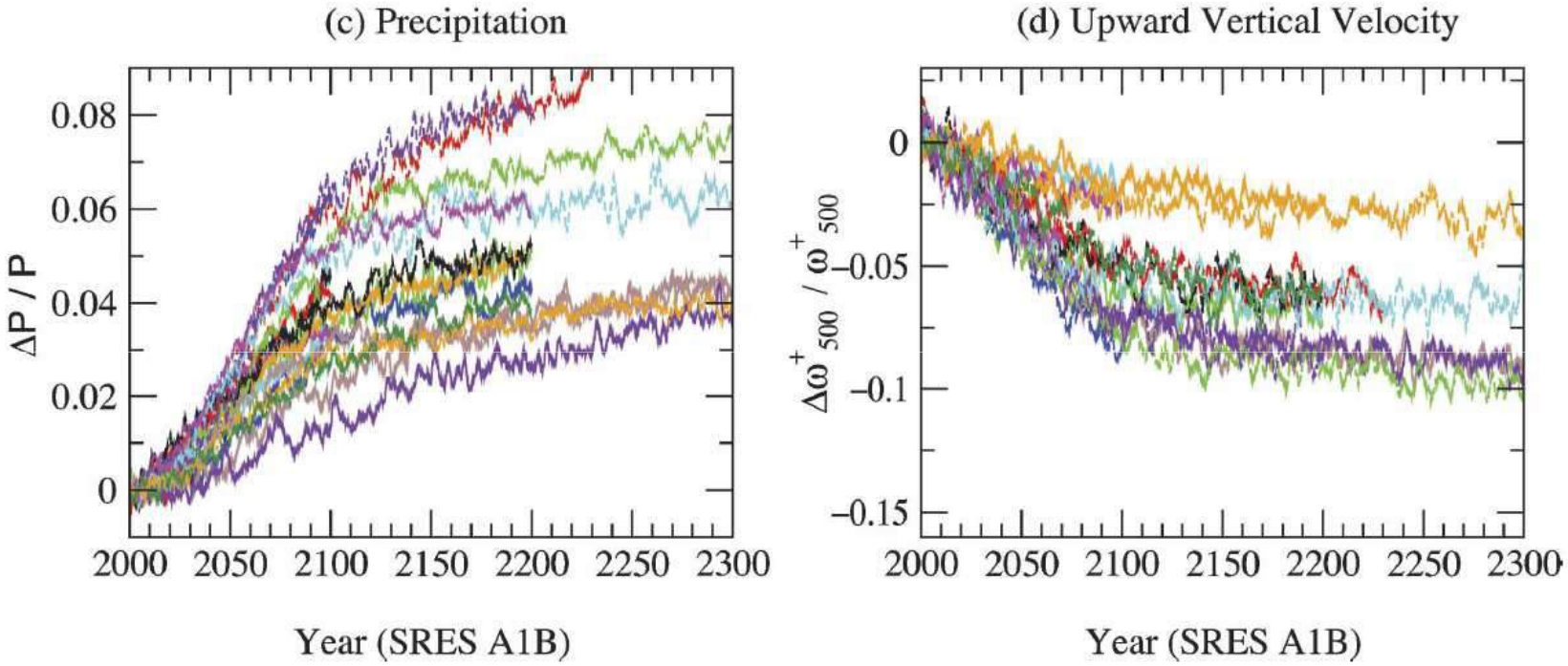

$$P = Mq \qquad \frac{\Delta M}{M} = \frac{\Delta P}{P} - \frac{\Delta q}{q} < 0$$

Held and Soden (2006) JCLI

Weakening of Tropical Circulation

Sugi et al. 2002, JMSJ

Table 2. Variables related to tropical circulation

Variables	CNTL	2xCO2	Difference %
Precipitation	3.43	3.47	+ 1.0
Evaporation	3.78	3.83	+ 1.4
Radiative Cooling	101.0	102.0	+ 1.0
Stability	47.2	49.8	+ 5.5
Mass flux	1.429	1.337	- 6.4
Precipitable Water	3.35	3.81	+ 13.7

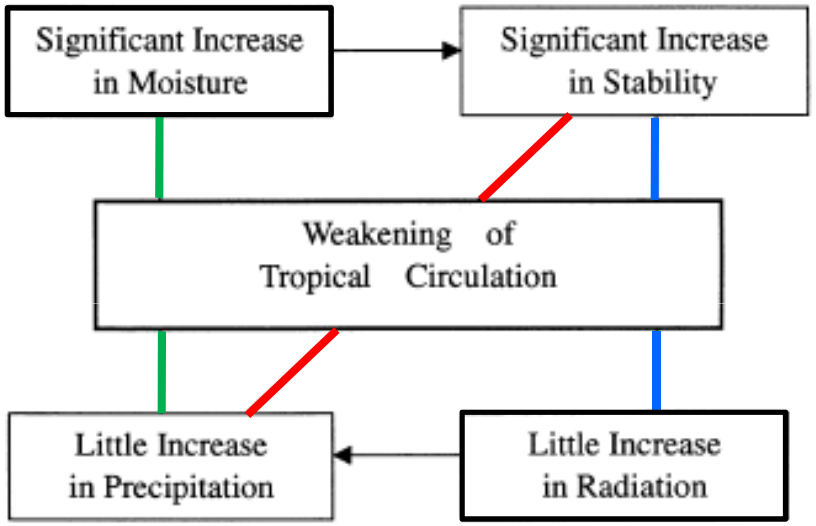

$$MS = Q$$

$$Mq = P$$

水蒸気が増えると大気の(乾燥)安定度が増加する

$$\Delta T = \frac{L}{C_p} q_B$$

$$\Delta\theta = \Delta T \left(\frac{p_0}{p} \right)^{\frac{R}{C_p}} \propto q_B$$

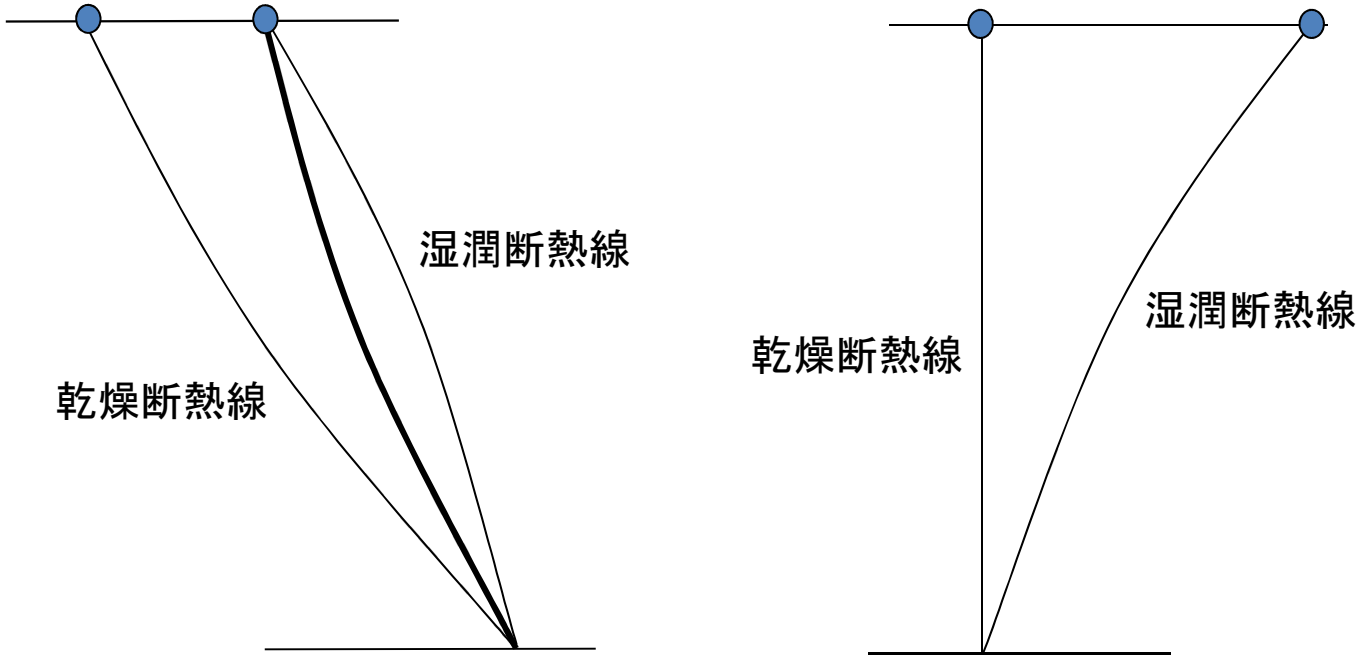

$$\text{安定度} \quad \propto \quad \Delta\theta \quad \propto \quad q_B$$

Sugi and Yoshimura (2004) JCLI

NOTES AND CORRESPONDENCE

A Mechanism of Tropical Precipitation Change due to CO_2 Increase

MASATO SUGI

Meteorological Research Institute, Tsukuba, Japan

JUN YOSHIMURA

Frontier Research System for Global Change, Yokohama, Japan

13 February 2003 and 15 July 2003

ABSTRACT

A recent GCM study indicates that a weakening of tropical circulation associated with a slight increase in tropical precipitation may occur when atmospheric CO_2 is increased. To further understand the mechanism of atmospheric temperature and precipitation changes associated with the greenhouse gas increase, a numerical experiment was conducted using an atmospheric general circulation model to investigate the separate effects of CO_2 increase and sea surface temperature (SST) increase. It has been shown that the effect of CO_2 increase is a reduction of radiative cooling in the lower troposphere, leading to a reduction of tropical precipitation. When atmospheric CO_2 concentration is doubled (quadrupled) without changing the SST, the tropical precipitation is reduced by about 3% (6%) in the model. The reduction of radiative cooling is a result of the overlap effect of the CO_2 15-μm and water vapor absorption bands. On the other hand, the effect of SST increase is the increase in atmospheric temperature and water vapor, leading to increases in radiative cooling and tropical precipitation. When SST is uniformly raised 2°C without changing the atmospheric CO_2 concentration, the tropical precipitation is increased by about 6%.

Sugi and Yoshimura (2004) JCLI

二酸化炭素と水蒸気の赤外放射の
吸収帯の重なり（オーバーラップ効果）

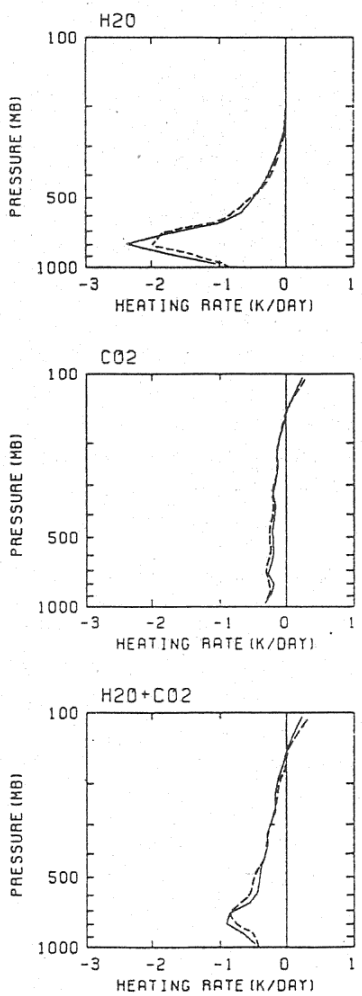

二酸化炭素の増加

➡ 放射冷却の減少

➡ 降水量の減少

降水量の減少　　放射冷却の減少

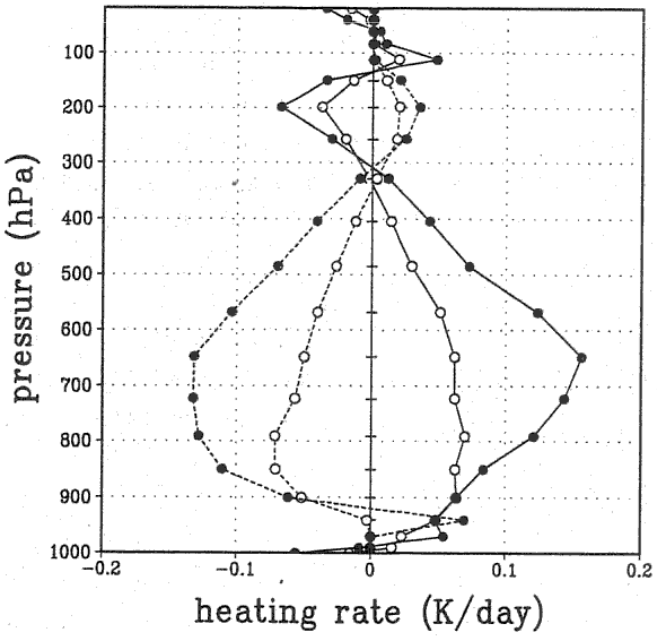

Allen and Ingram (2002) Nature

CO2を2倍にしたときの気温の変化と降水量の変化

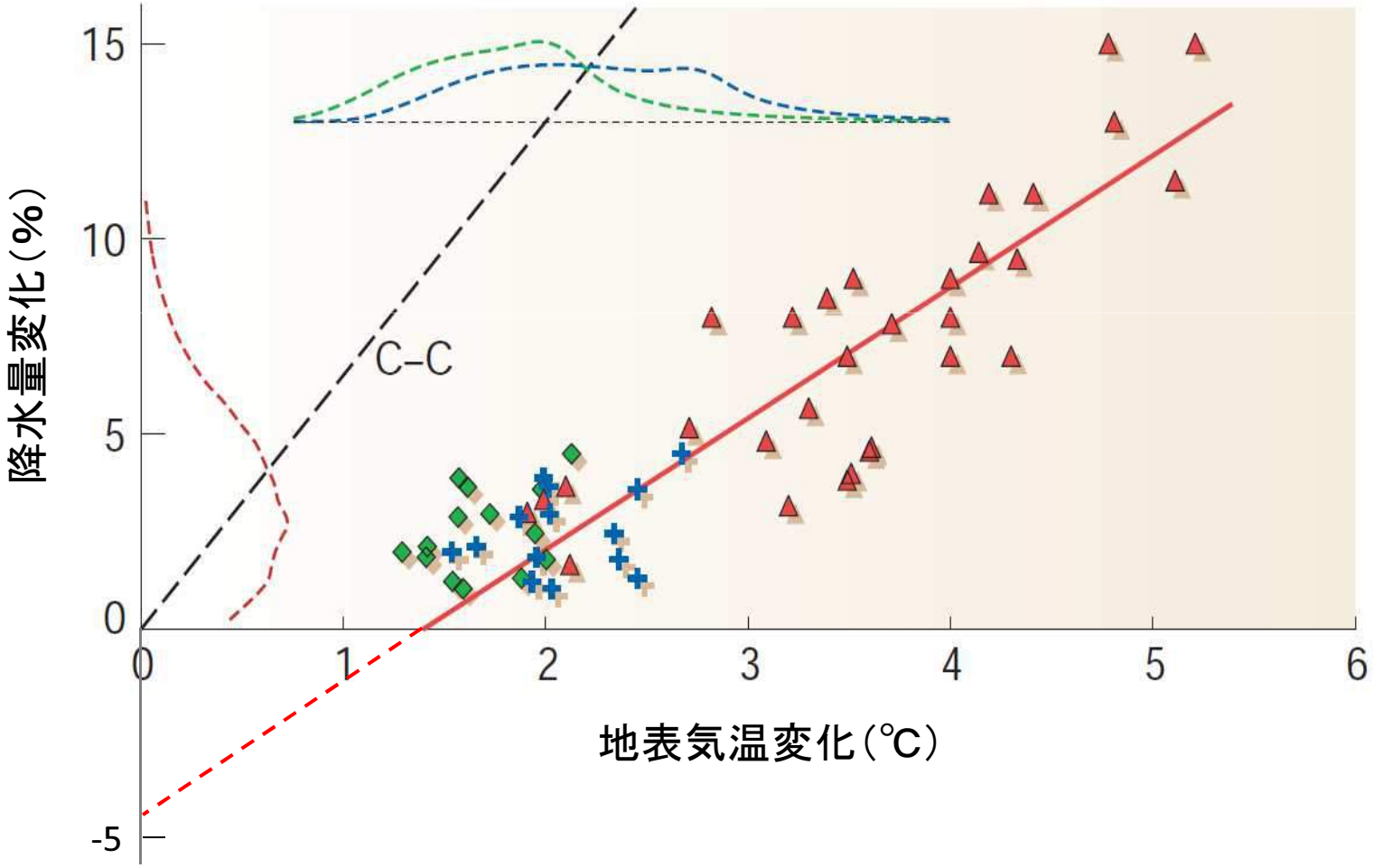

熱帯大気循環（積雲対流）の模式図

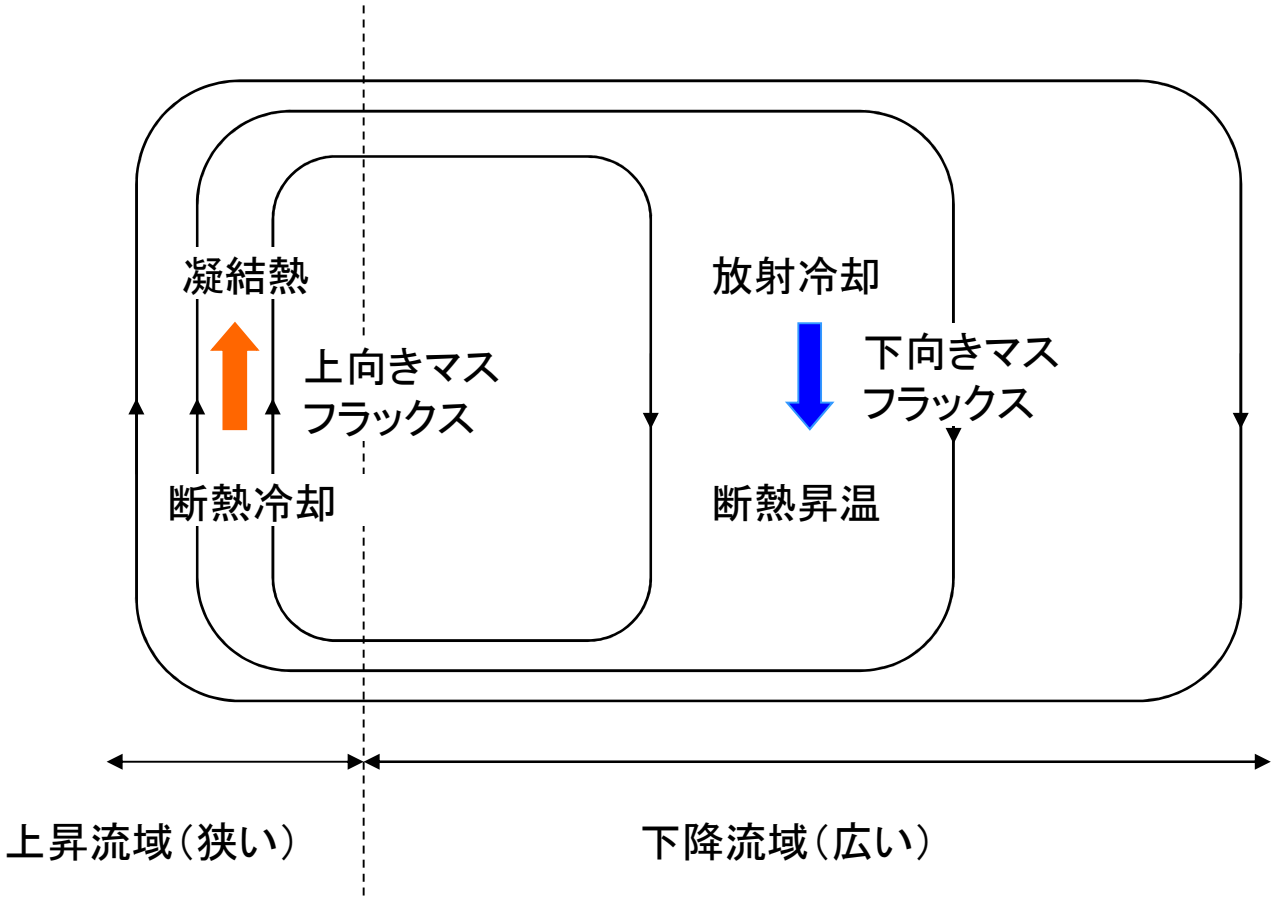

マスフラックス　x　安定度　＝　加熱　(冷却)

Upward mass flux hypothesis (Sugi)

温暖化すると台風が減る理由

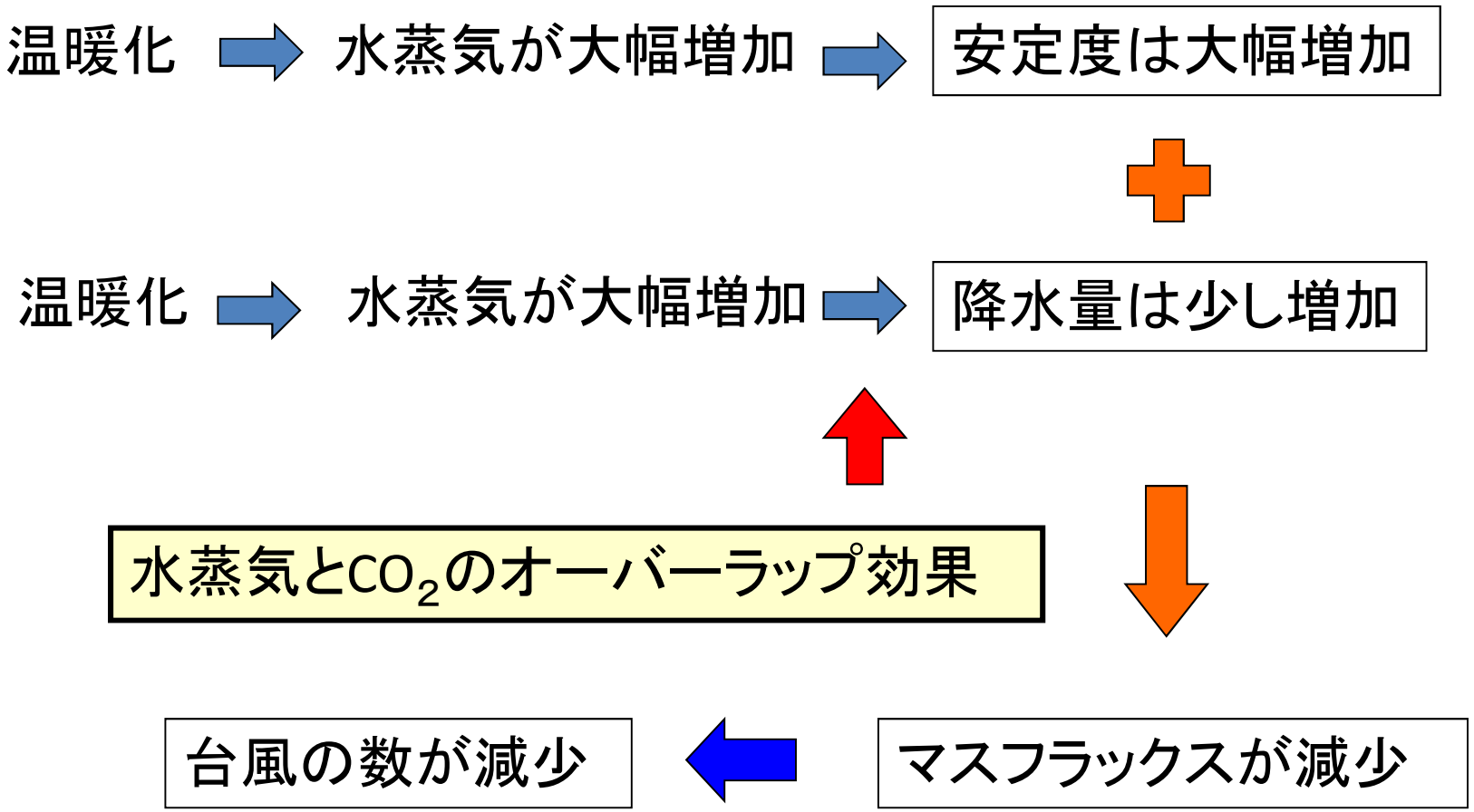

Emanuel et al. (2008) BAMS

Saturation deficit hypothesis (Emanuel)

Warming → q* increase

→ q*-q (saturation deficit) increase

→ unfavorable for TC genesis

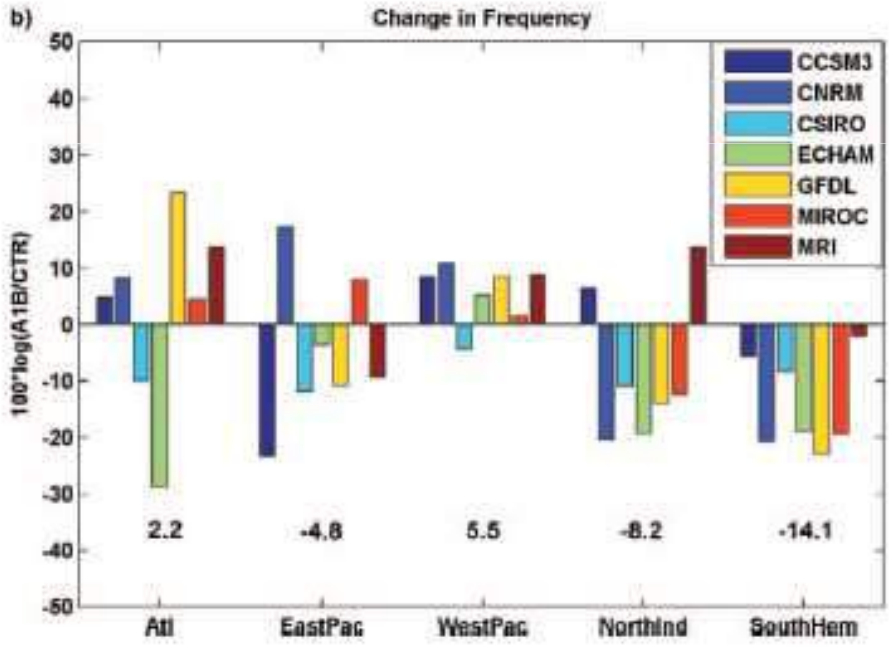

q* variable

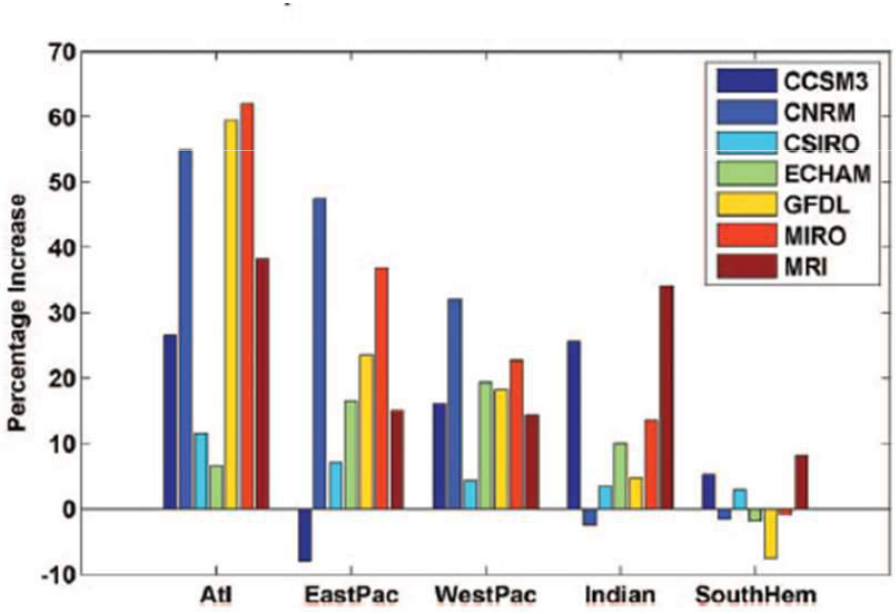

q* constant

Rappin et al. (2010) QJRMS

Nolan (2004) developed a more generalized index to relate past, present, and future climate states to TC activity:

$$GP = |10^5\eta|^{\frac{3}{2}}(\frac{H}{50})^3(\frac{V_{pot}}{70})^3(1+0.1V_{shear})^{-2}. \quad (1)$$

where η is the absolute vorticity, H is the mid-level relative humidity, V_{pot} is the potential intensity as defined by Bister and Emanuel (2002), and V_{shear} is the 850-200 hPa vertical shear. The index is able to reproduce seasonal variations in both hemispheres, and Camargo et al. (2007) showed that it is able to capture inter-annual variations, particularly those associated with ENSO. Despite these successes, the index suffers from several flaws. Most glaring is its dimensional inconsistency. Moreover, recent studies by Nolan et al. (2007 - hereafter N07) and Nolan and Rappin (2008 - hereafter N08) showed that the index predicted an increase in genesis in an environment of increasing SST, whereas numerous GCM simulations with and without regional downscaling show a general decrease in genesis with increasing SST due to global warming (Sugi et al. 2002; Yoshimura et al. 2006; Bengtsson et al. 2007; Emanuel et al. 2008; Knutson et al. 2008), albeit with much regional variability.

Rappin et al. (2010) QJRMS

candidate parameter. Recently, E08 discussed the quantity χ_m, an important parameter of Emanuel's Coupled Hurricane Intensity Prediction System (CHIPS) model (Emanuel et al. 2004), the magnitude of which may correlate well with the approximate timescale for intensification of an incipient tropical cyclone-like disturbance. It is defined as:

$$\chi_m = \frac{s_b - s_m}{s_0^* - s_b}. \tag{2}$$

Here s_m, s_b, and s_0^* are the moist entropies of the mid-troposphere, the boundary layer, and the sea surface at saturation, respectively. The moist entropy is approximately (Emanuel 1994)

$$s = c_p \ln T - R_d \ln p + \frac{L_v q}{T} - R_v q \ln H, \tag{3}$$

where c_p and R_d are the heat capacity and gas constant of dry air, respectively. R_v is the gas constant for water vapor, L_v is the latent heat of vaporization, q is the specific humidity, and H is the relative humidity.

$$s_m^* - s_m \approx L_v \frac{q_m^* - q_m}{T_m}, \tag{4}$$

where the subscripts m denote evaluation in the middle troposphere. This shows that the inhibiting effect of middle troposphere dryness scales as the saturation deficit, not as the relative humidity per se. This suggests that relative humidity used in the earlier definition of GP given by (1) should be replaced by the saturation deficit, or by its non-dimensional equivalent given by χ_m. Of course, as long as the temperature of the middle troposphere is approximately constant in space and time, calibrating (1) on variations in the current climate cannot reveal the deficiency of using relative humidity in place of saturation deficit.

I. なぜ地球温暖化により台風の数が減るのか

(2) CO2 effect and SST effect

Yoshimura and Sugi (2005) SOLA
Held and Zhao (2011)
Sugi et al. (2012)
Sugi and Yoshimura (2012)
Emanuel (2013)
杉ほか(2014) 気象学会

Yoshimura and Sugi (2005) SOLA

Tropical Cyclone Climatology in a High-resolution AGCM —Impacts of SST Warming and CO_2 Increase—

Jun Yoshimura[1] and Masato Sugi[2]
[1]*Frontier Research Center for Global Change, Yokohama, Japan*
[2]*Meteorological Research Institute, Tsukuba, Japan*

Table 1. Summary of the numerical experiments. The same as those of SY2004.

Experiment	SST	CO_2 concentration
COOL1	2 K cooling	Normal
CLIM1	Climatology	Normal
WARM1	2 K warming	Normal
WARM2	2 K warming	2 x CO_2
WARM4	2 K warming	4 x CO_2

Yoshimura and Sugi (2005) SOLA

海面水温だけ、または、CO2だけを増加させたときの台風の数の変化

Table 4. Changes in precipitation and dry static stability, averaged between 30°S and 30°N, and changes in global frequencies of TC genesis. Dry static stability is defined as difference in potential temperature between 250 hPa and the surface (SY2004).

[SST effect]	Change (relative to CLIM1)		
	Precipitation	Stability	TC frequency
COOL1	−5.6%	−9.6%	−0.1%
WARM1	+6.1%	+9.4%	−12.4%

[CO_2 effect]	Change (relative to WARM1)		
	Precipitation	Stability	TC frequency
WARM2	−3.0%	+0.2%	−13.4%
WARM4	−6.3%	+0.4%	−44.1%

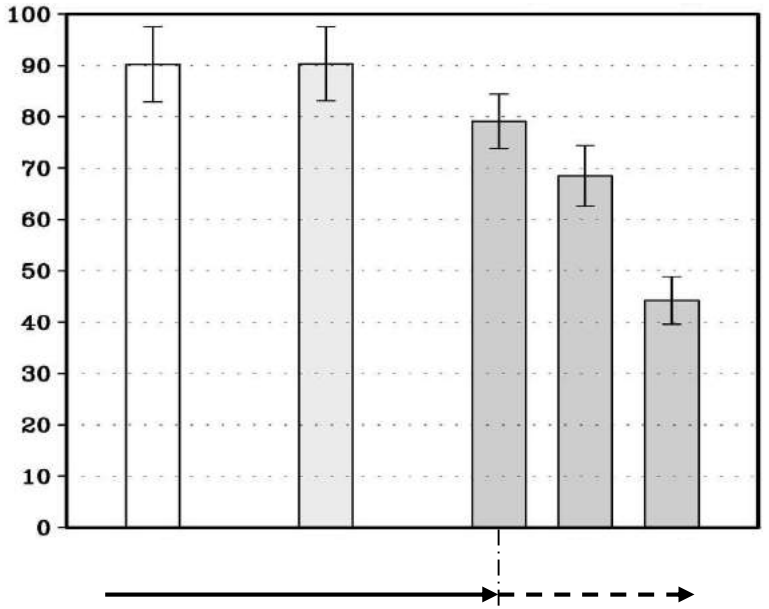

海面水温増加　CO2増加

降水量増加　降水量減少

安定度増加　安定度変化なし

Held and Zhao (2011) JCLI

The Response of Tropical Cyclone Statistics to an Increase in CO_2 with Fixed Sea Surface Temperatures

ISAAC M. HELD

NOAA/Geophysical Fluid Dynamics Laboratory, Princeton, New Jersey

MING ZHAO

NOAA/Geophysical Fluid Dynamics Laboratory, Princeton, New Jersey, and University Corporation for Atmospheric Research, Boulder, Colorado

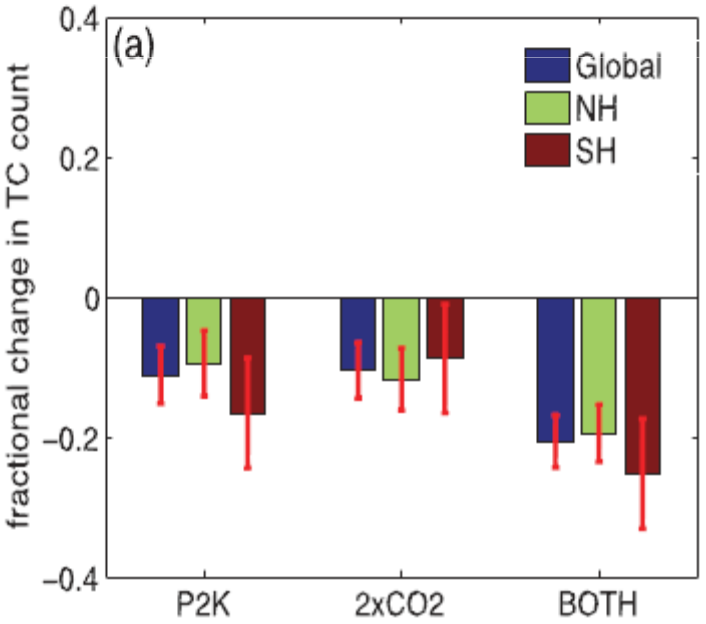

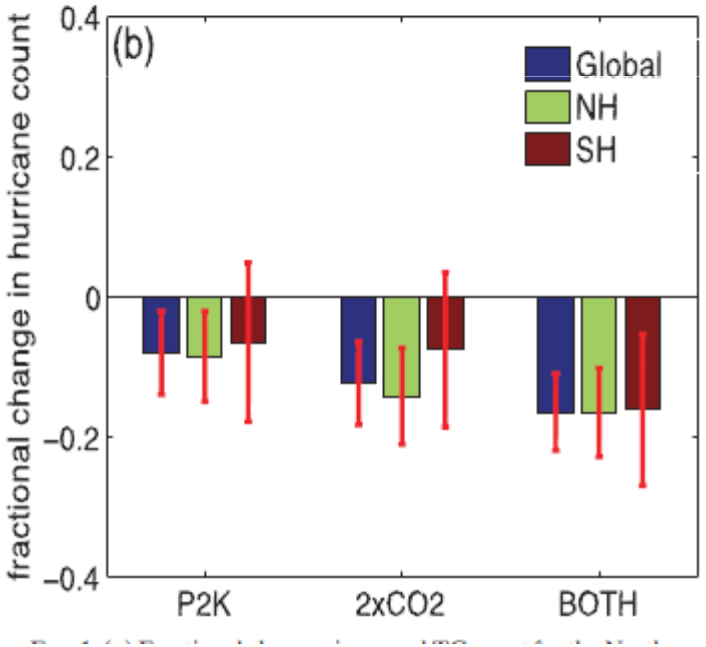

Held and Zhao (2011) JCLI

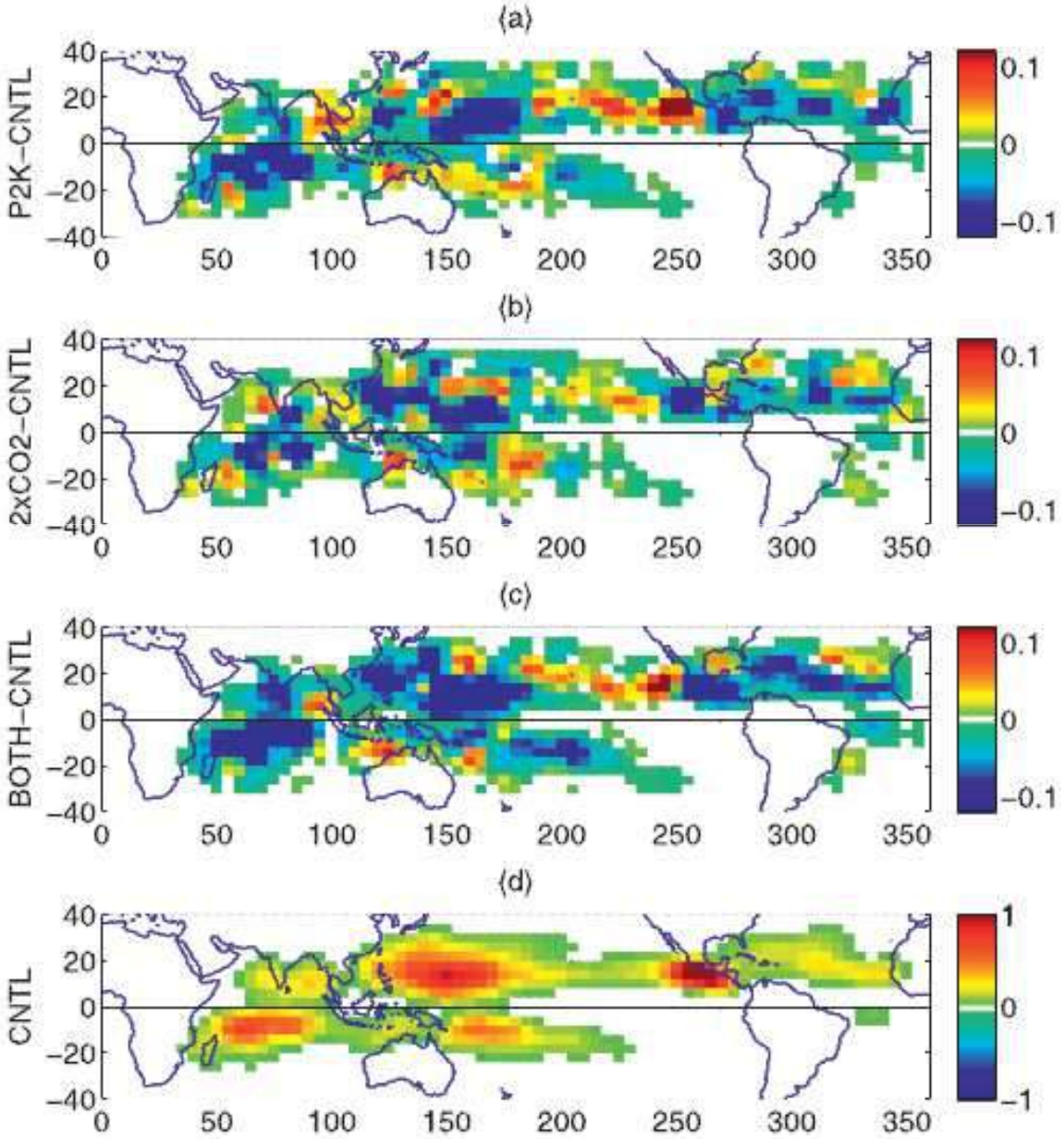

Held and Zhao (2011) JCLI

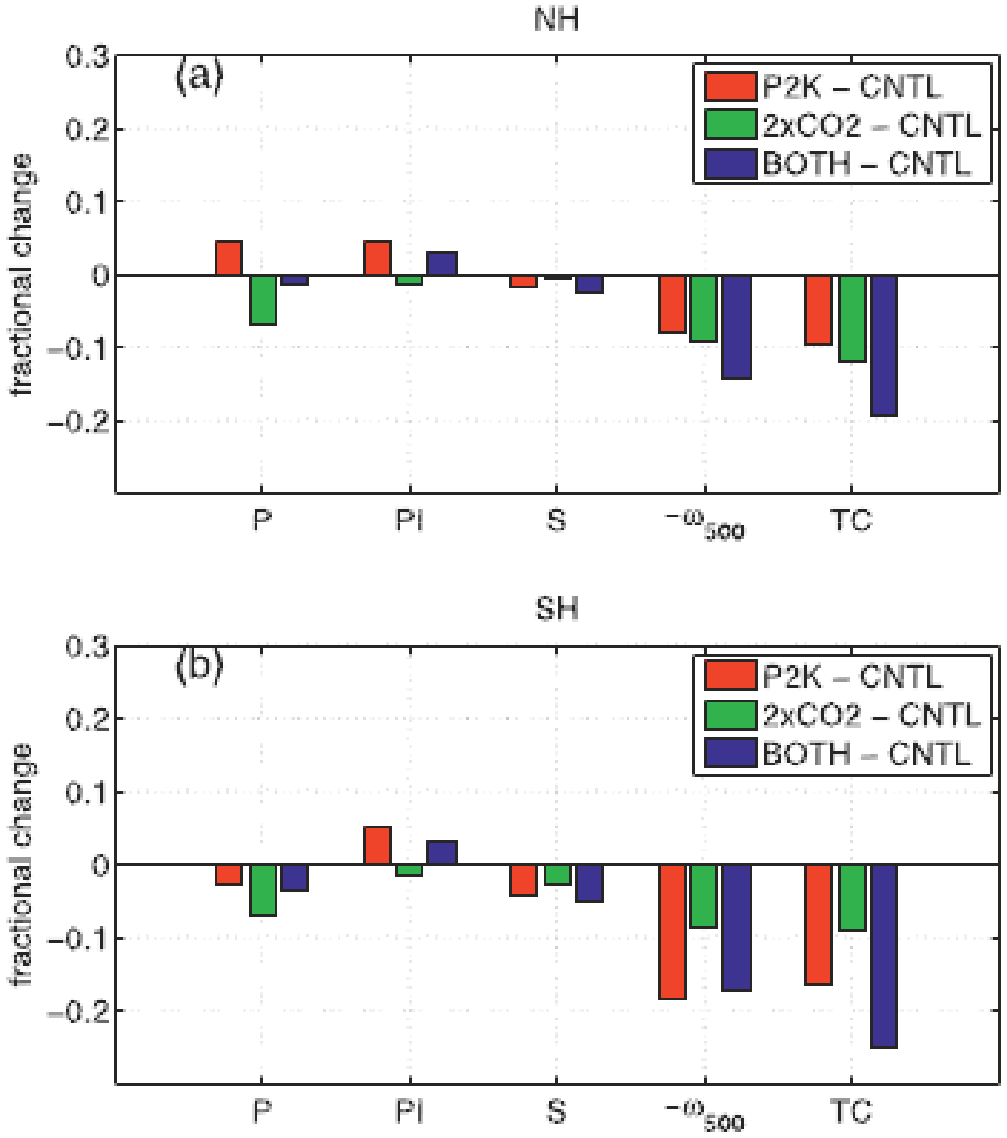

Held and Zhao (2011) JCLI

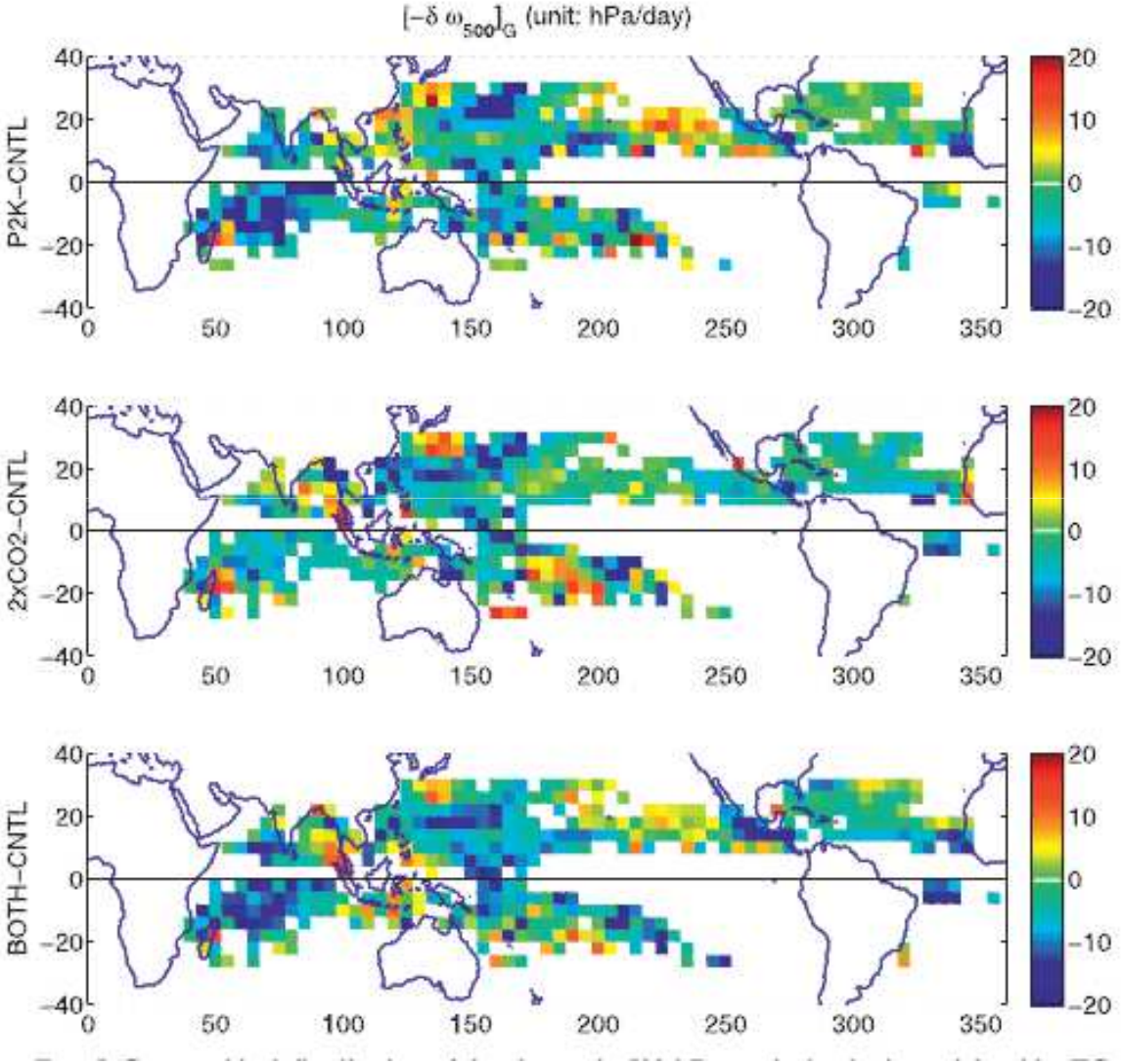

Zhao (2013) US CLIVAR WS

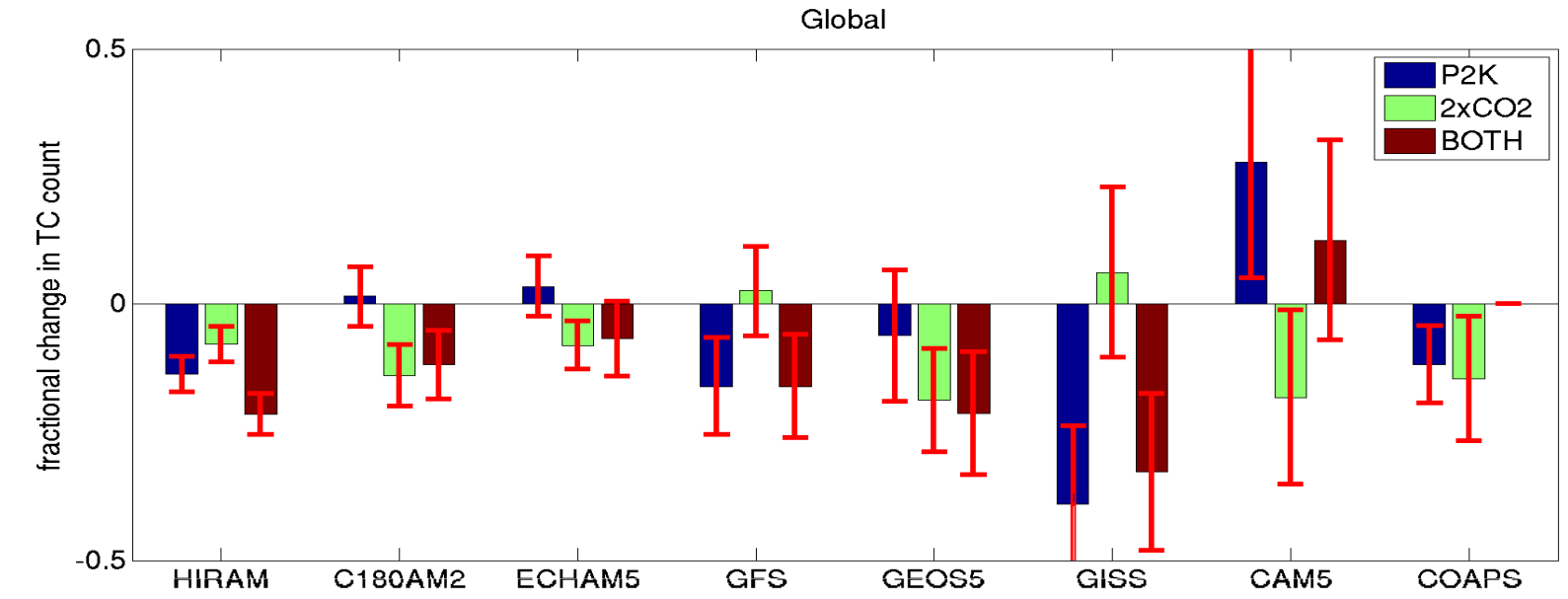

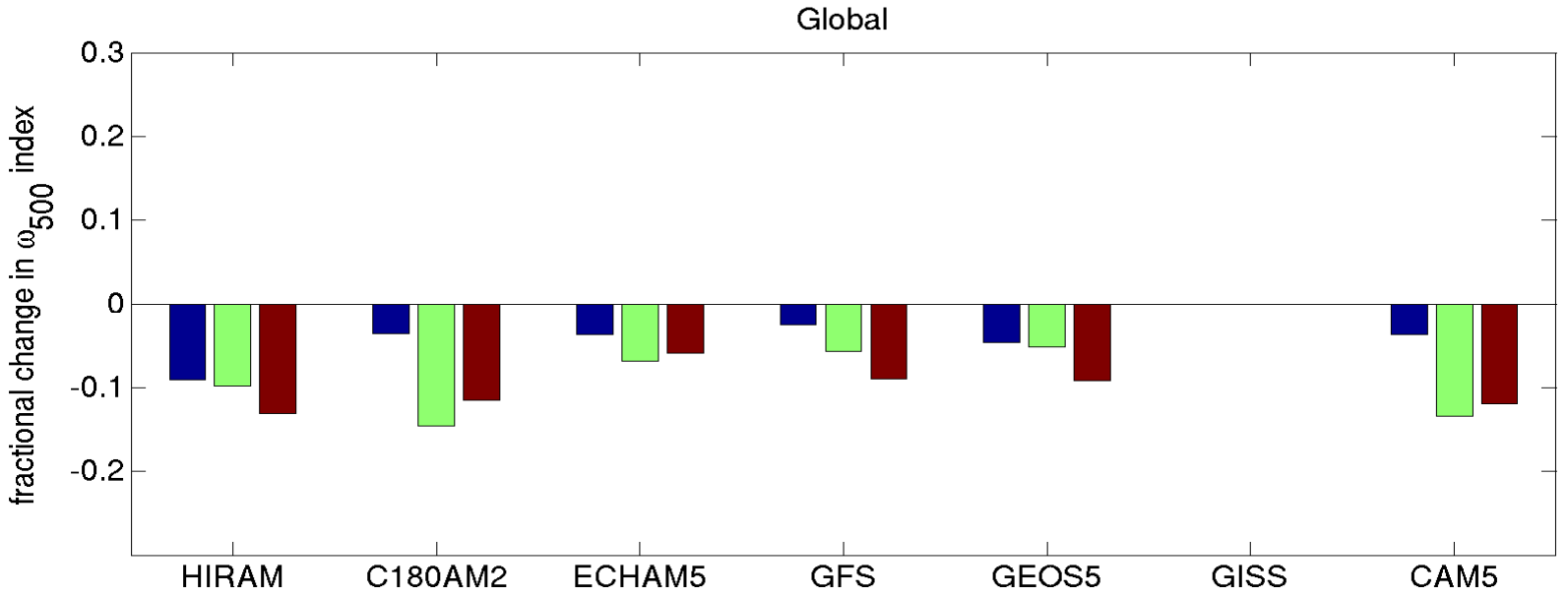

Sugi et al. (2012) JMSJ

NOTES AND CORRESPONDENCE

On the Mechanism of Tropical Cyclone Frequency Changes Due to Global Warming

Masato SUGI, Hiroyuki MURAKAMI

Japan Agency for Marine-Earth Science and Technology, Yokohama, Japan

and

Jun YOSHIMURA

Meteorological Research Institute, Tsukuba, Japan

Table 1. Experiments.

Name (Short Name)	Experiment (Run)	SST	GHG
HPA (P)	Present day climate simulation 1979–2003	Present	Present
HFA (F)	Future climate simulation 2075–2099	Future	Future
CO2F (CF)	Future CO2 simulation 2075–2099	Present	Future
SSTF (SF)	Future SST simulation 2075–2099	Future	Present

Sugi et al. (2012) JMSJ

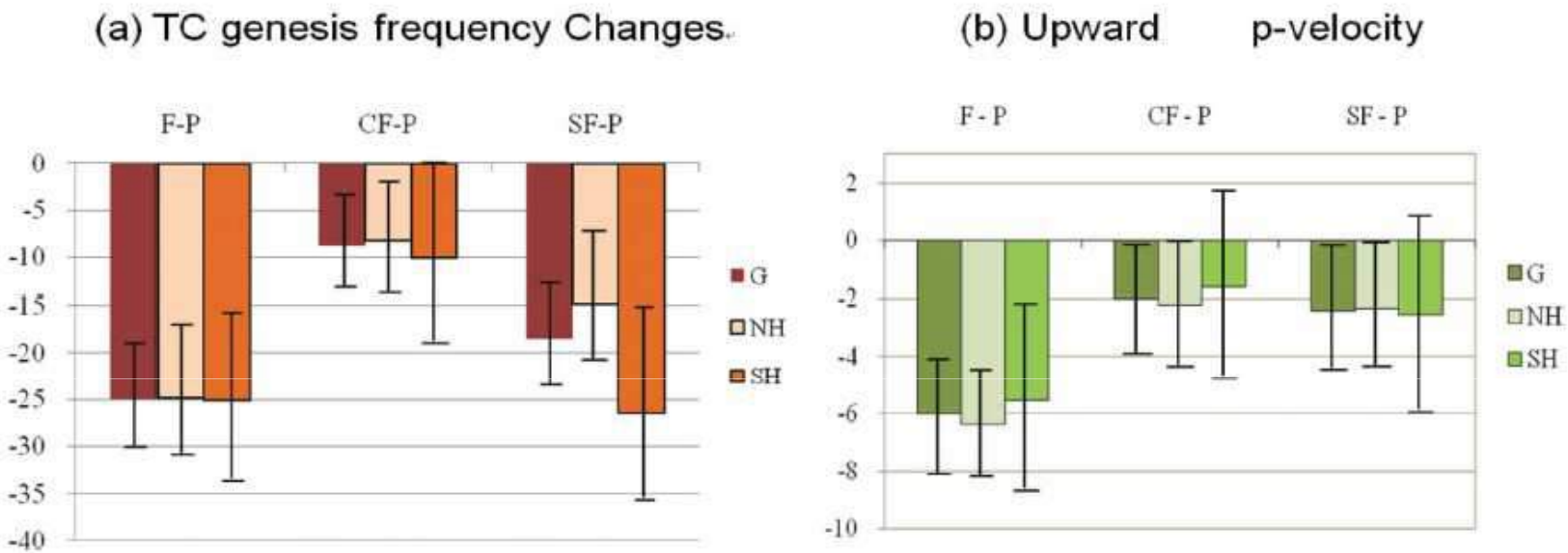

Fig. 1. (a) TC frequency changes of HF (F), CO2F (CF) and SSTF (SF) runs from HPA (P) run. Unit is %. (b) Same as (a) but for upward mass flux (*p*-velocity) at 500 hPa averaged over the tropical ocean (5°N–30°N, 5°S–30°S) and respective TC season (NH: JUN–NOV, SH: JAN–APR). Error bars indicate the 90% confidence interval estimated by *t*-test.

Sugi et al. (2012) JMSJ

flux changes? Over the precipitating area in the tropics, an approximate form of thermodynamic equation can be written as

$$\omega S \approx \alpha P, \tag{1}$$

where α is a scaling constant (Holton 1979). If the temporal and spatial variation of S is small, compared with the variation of ω and P, then the equation also holds for area mean or time mean of ω and P. From Eq. (1), we can derive a following relation for fractional changes of P, ω and S.

$$\frac{\Delta\omega}{\omega} \approx \frac{\Delta P}{P} - \frac{\Delta S}{S}. \tag{2}$$

Table 3. Fractional changes in precipitation (P), upward mass flux at 500 hPa (ω), their difference and dry static stability at 500 hPa (S) averaged over the tropical ocean (5°N–30°N, 5°S–30°S) and respective TC season (NH: JUN–NOV, SH: JAN–APR). Unit is %.

		$\frac{\Delta P}{P}$	$\frac{\Delta\omega}{\omega}$	$\frac{\Delta P}{P} - \frac{\Delta\omega}{\omega}$	$\frac{\Delta S}{S}$
NH	F–P	5.8	−6.4	12.2	12.1
	CF–P	−3.8	−2.2	−1.6	0.0
	SF–P	10.5	−2.3	12.8	12.2
SH	F–P	5	−5.5	10.5	11.2
	CF–P	−4.4	−1.6	−2.8	0.0
	SF–P	9	−2.5	11.5	11.0

Sugi et al. (2012) JMSJ

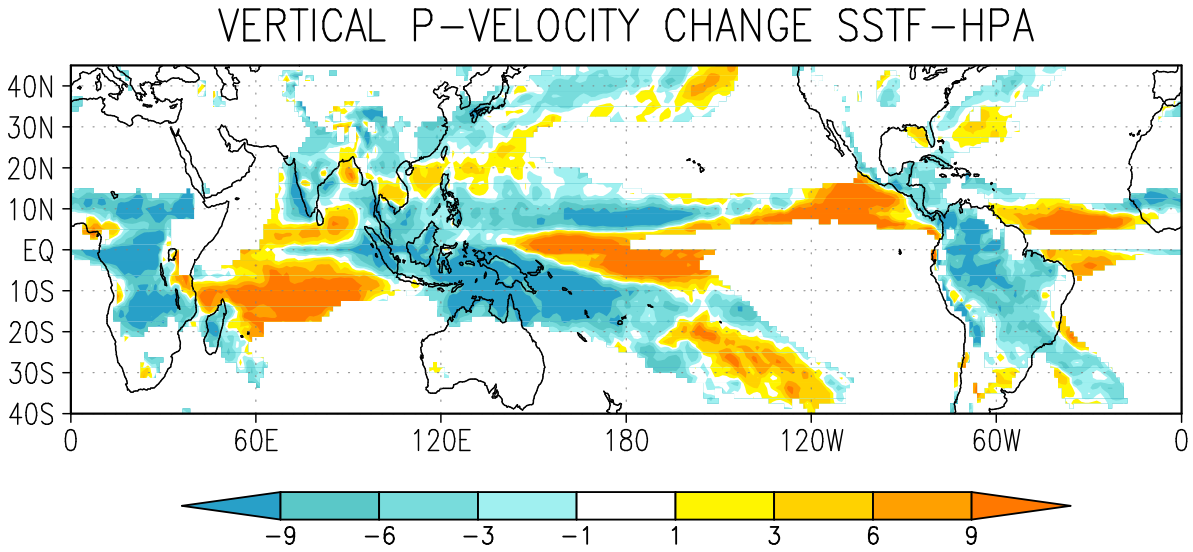

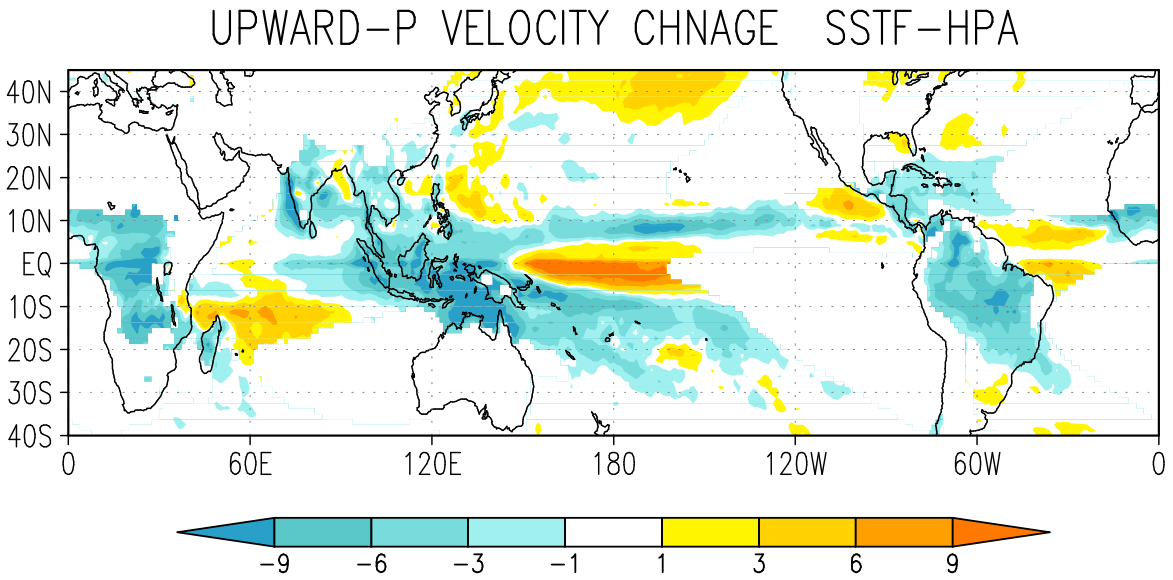

$$\frac{\Delta \omega}{\omega} \approx \frac{\Delta P}{P} - \frac{\Delta S}{S}$$

Sugi et al. (2013)
Kakushin WS

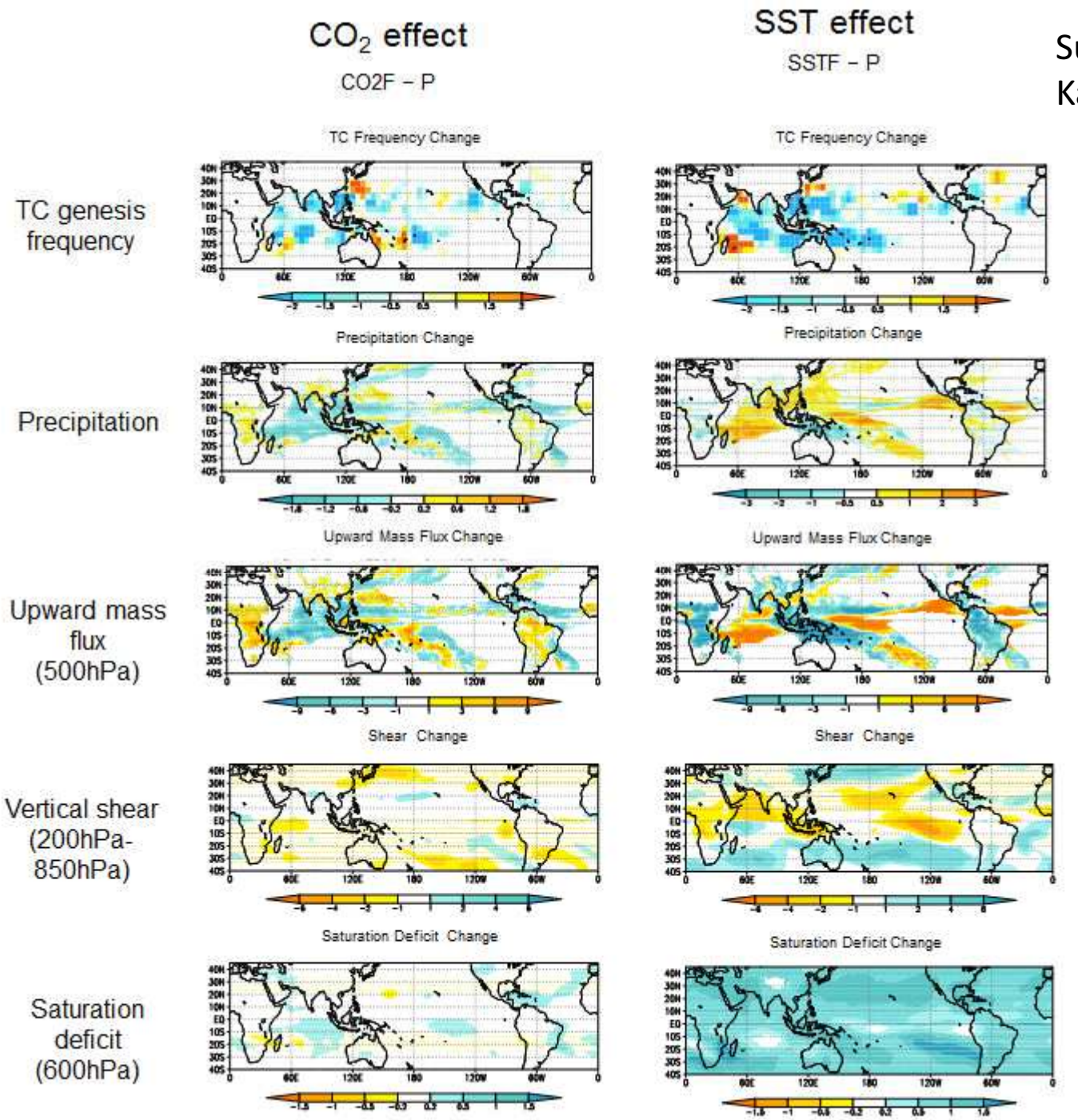

Sugi et al. (2013) Kakushin WS

4. Uniform SST effect and non-uniform SST effect

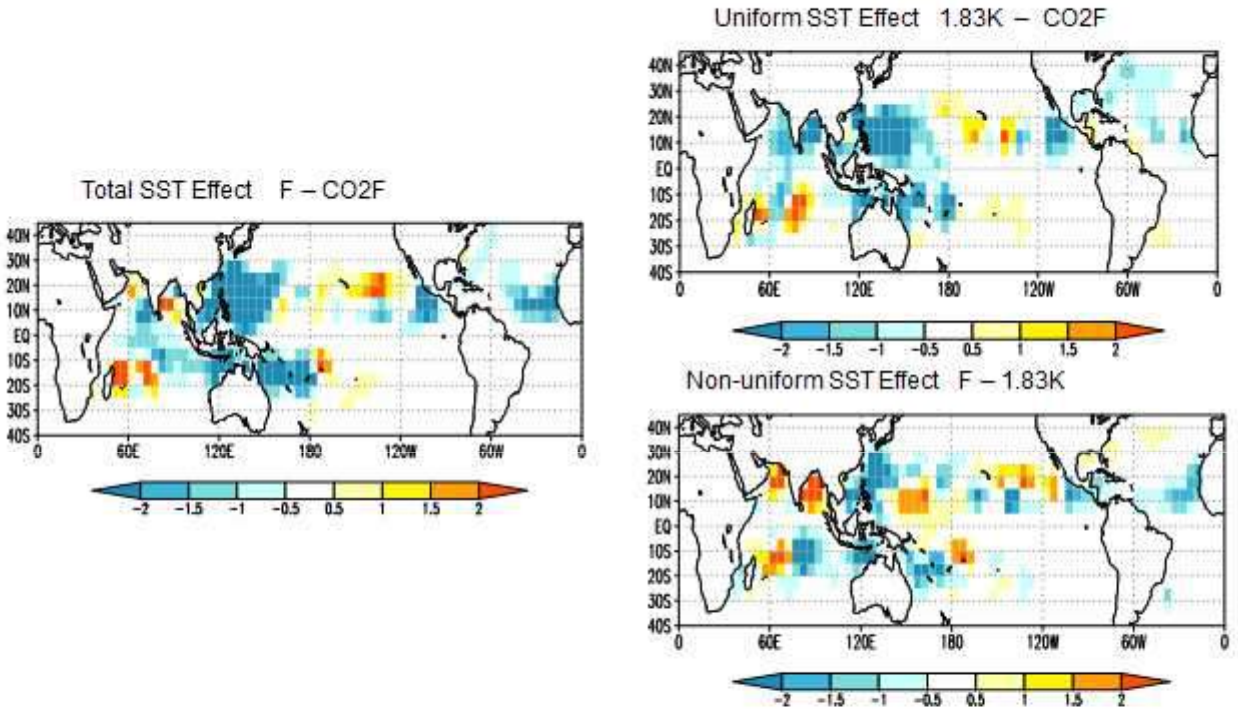

- Non-uniform SST effect (effect of SSTA relative to the mean tropical SSTA) is mainly responsible for the regional TC frequency changes.
- Non-uniform SST effect causes little change in global TC frequency. It only causes shifts of active convection areas, leading to shifts of TC genesis area.

Sugi et al. (2013) Kakushin WS

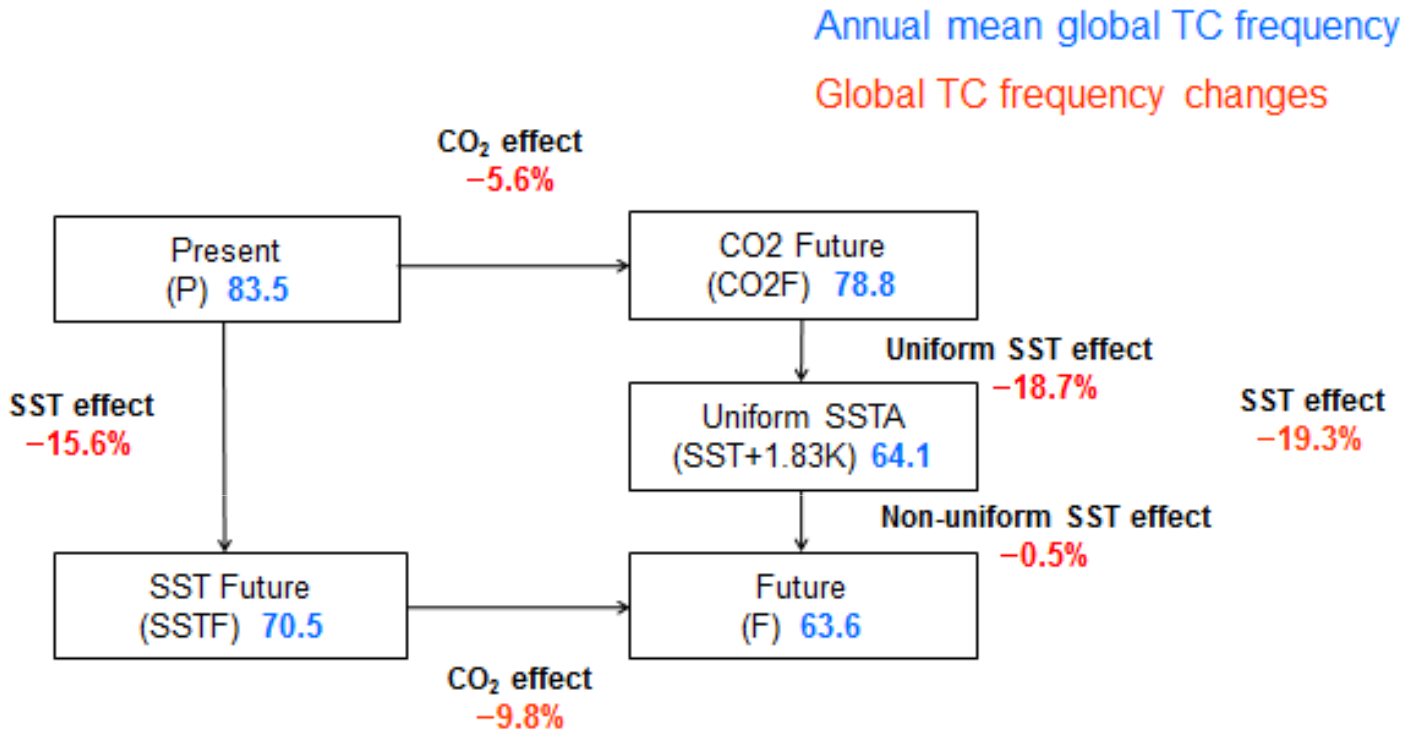

- Five 25year runs are conducted using the MRI-AGCM3.2 with 60km resolution.
- Observed SST (1979-2003) is prescribed for the present climate run, while CMIP3 ensemble mean SSTA (2075-2099) is added and GHG is changed according to IPCC A1B scenario in the future climate run.

2. Mechanism of TC frequency changes (Hypothesis)

Sugi et al. (2013)
Kakushin WS

Effect		Global change					Regional change
		Radiative cooling	Precipitation	Stability	Upward mass flux	TC frequency	TC frequency
CO_2	CO_2	Decrease	Decrease		Decrease	Decrease	
	Other GHG	Increase	Increase		Increase	Increase	
SST	Uniform SSTA	Increase	Increase	Increase	Decrease	Decrease	
	Non-uniform SSTA						Shift

- We have noted that the changes in global TC frequency are closely related to the changes in upward mass flux.
- We consider CO_2 effect and SST effect for the reduction of upward mass flux and TC frequency.
- The overlap effect of CO_2 and H_2O long wave radiation absorption bands is playing an important role in the CO_2 effect.
- Stability effect is playing an important role in the SST effect.
  From thermodynamic equation $\omega S \approx \alpha P$ (α is a scaling constant), we can derive a relation:

$$\frac{\Delta\omega}{\omega} \approx \frac{\Delta P}{P} - \frac{\Delta S}{S}$$

ω : upwarad mass flux
P : precipitation
S : dry static stability

Sugi and Yoshimura (2012) GRL

Decreasing trend of tropical cyclone frequency in 228-year high-resolution AGCM simulations

Masato Sugi[1,2] and Jun Yoshimura[2]

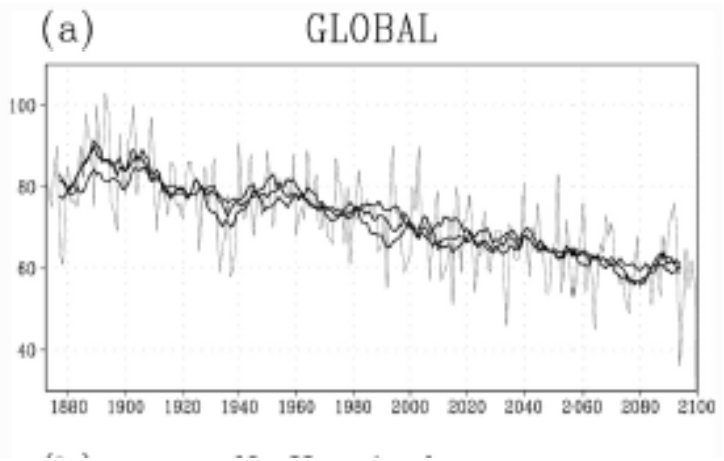

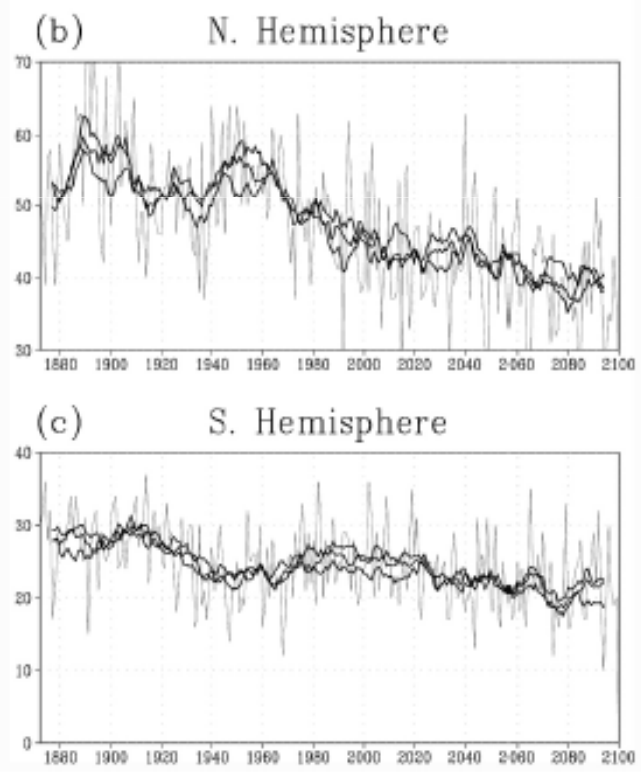

Sugi and Yoshimura (2012) GRL

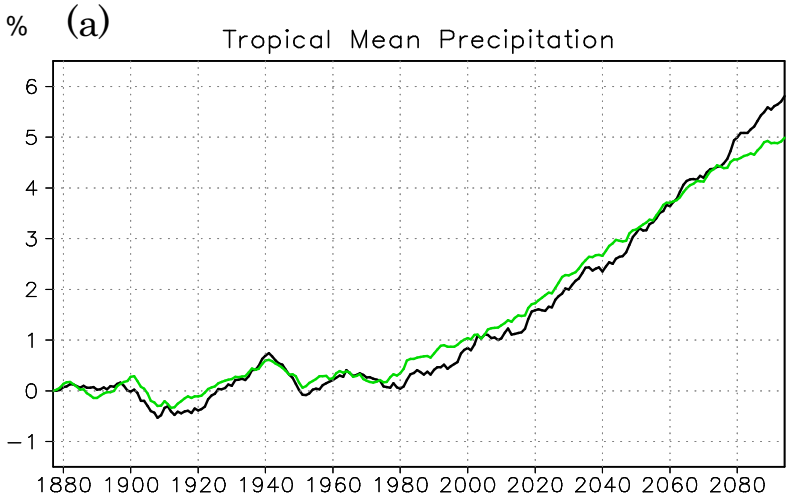

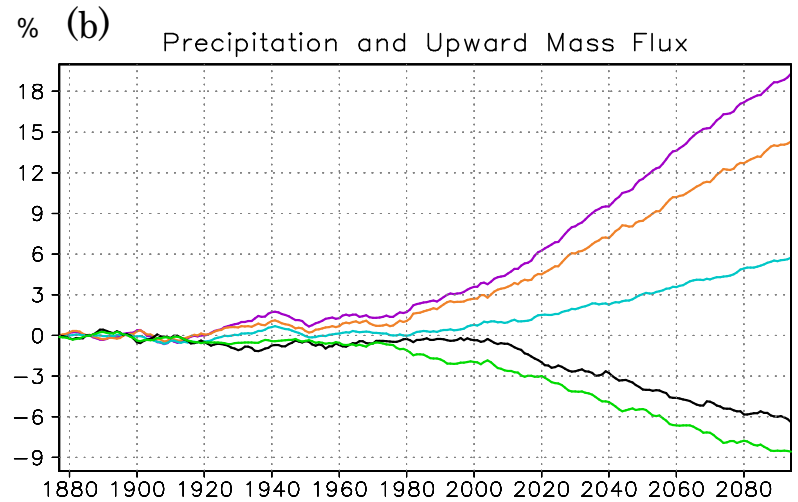

降水量、安定度、上昇流の変化

$$\Delta R = a\Delta T - b\Delta C$$

$$P \approx \alpha\omega\, S$$

$$\frac{\Delta\omega}{\omega} \approx \frac{\Delta P}{P} - \frac{\Delta S}{S}$$

Fig. S2 (a) Same as in Fig. S1c, but for the tropics mean precipitation averaged between 30˚N and 30˚S. (b) Long-term fractional changes (anomaly from the first thirty year mean, unit is %) in surface specific humidity (purple line), dry static stability (orange line), precipitation (blue line), simulated upward mass flux (black line) and upward mass flux calculated by Eq. (S3) (green line).

Sugi and Yoshimura (2012) GRL

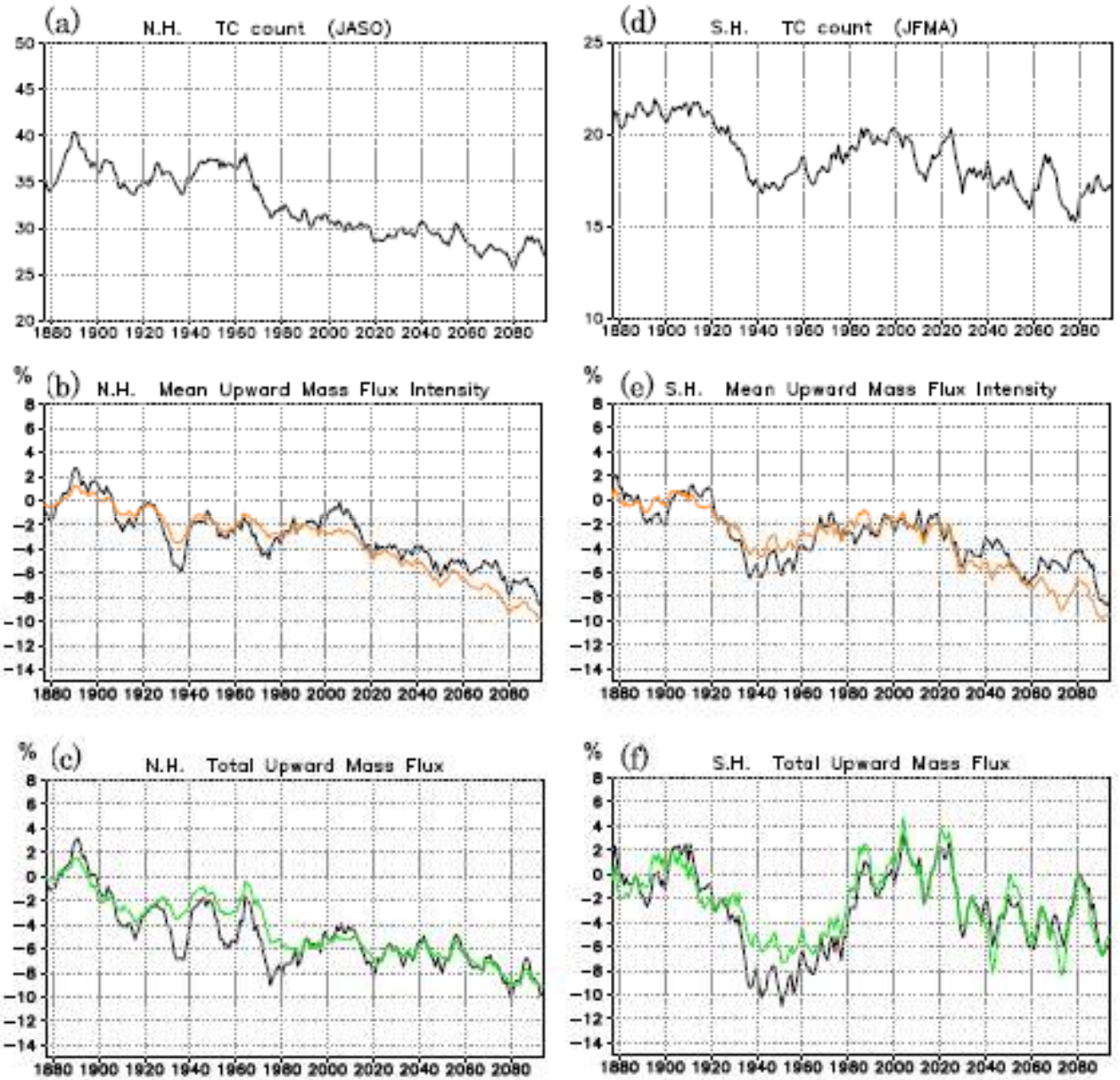

Emanuel (2013) PNAS

Downscaling CMIP5 climate models shows increased tropical cyclone activity over the 21st century

Kerry A. Emanuel[1]

Table 2. Comparison between CMIP3 and CMIP5 changes in downscaled tropical cyclone frequency and power dissipation

Institute ID	CMIP3 model	CMIP5 model	CMIP3 change in global frequency, %	CMIP5 change in global frequency, %	CMIP3 change in global power dissipation, %	CMIP5 change in global power dissipation, %
NCAR	CCSM3	CCSM4	−3	+11	+5	+8
GFDL	CM2.0	CM3	−13	+41	+2	+72
MOHC		HADGEM2-ES		+22		+31
MPI	ECHAM5	MPI-ESM-MR	−11	+29	+4	+57
MIROC	MIROC3.2	MIROC5	−12	+38	+8	+80
MRI	MRI-CGCM2.3.2a	MRI-CGCM3	+2	+13	+22	+26

For CMIP3 models, the listed numbers are percentage changes from the 20-y period 1981–2000 to the 20-y period 2181–2200 under emissions scenario A1b. For the CMIP5 models, the listed numbers represent percentage changes from 1981–2000 to 2081–2100 under radiative forcing scenario RCP8.5.

Emanuel (2013) PNAS

Constant seeding rate is assumed.

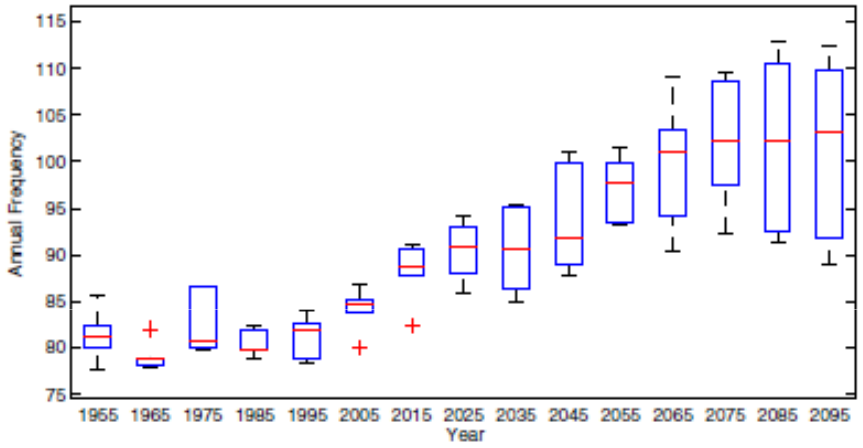

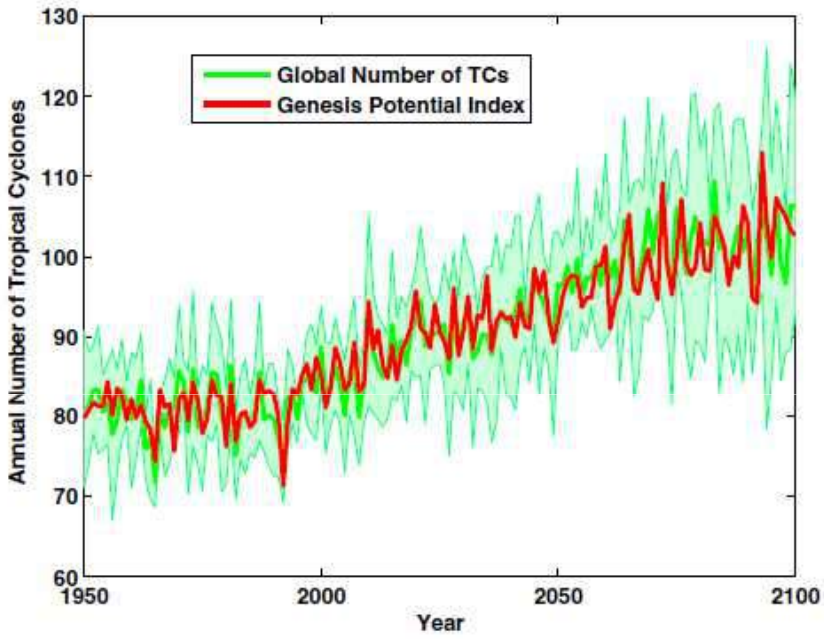

$$\chi = \frac{h^* - h_m}{h_0^* - h^*}$$

$$GPI \equiv |\eta|^3 \, \chi^{-4/3} \, Max((V_{pot} - 35\mathrm{m}\cdot\mathrm{s}^{-1}), 0)^2 \, (25\mathrm{m}\cdot\mathrm{s}^{-1} + V_{shear})^{-4}$$

地球が温暖化すると全球の台風の数が減る

Knutson et al. (2010)　Nature Geosci.

IPCC AR5 (2014)　Section 14.6.1　Fig.14.17

地球が寒冷化すると全球の台風の数は増える？

2014年度気象学会春季大会 （5月21日-24日横浜）　D159

寒冷化すると台風は増えるか？

杉　正人･吉田康平（気象研究所）

村上裕之（GFDL）

実験設定

・MRI-AGCM3.2： 水平解像度　60km (TL319)・鉛直64層

・SSTのみ変えて、それぞれ25年積分

実験	CO2	SST
現在気候	現在(1979-2003)	現在(1979-2003)
4K寒冷化	現在(1979-2003)	現在 – 4K
4K温暖化	現在(1979-2003)	現在 + 4K

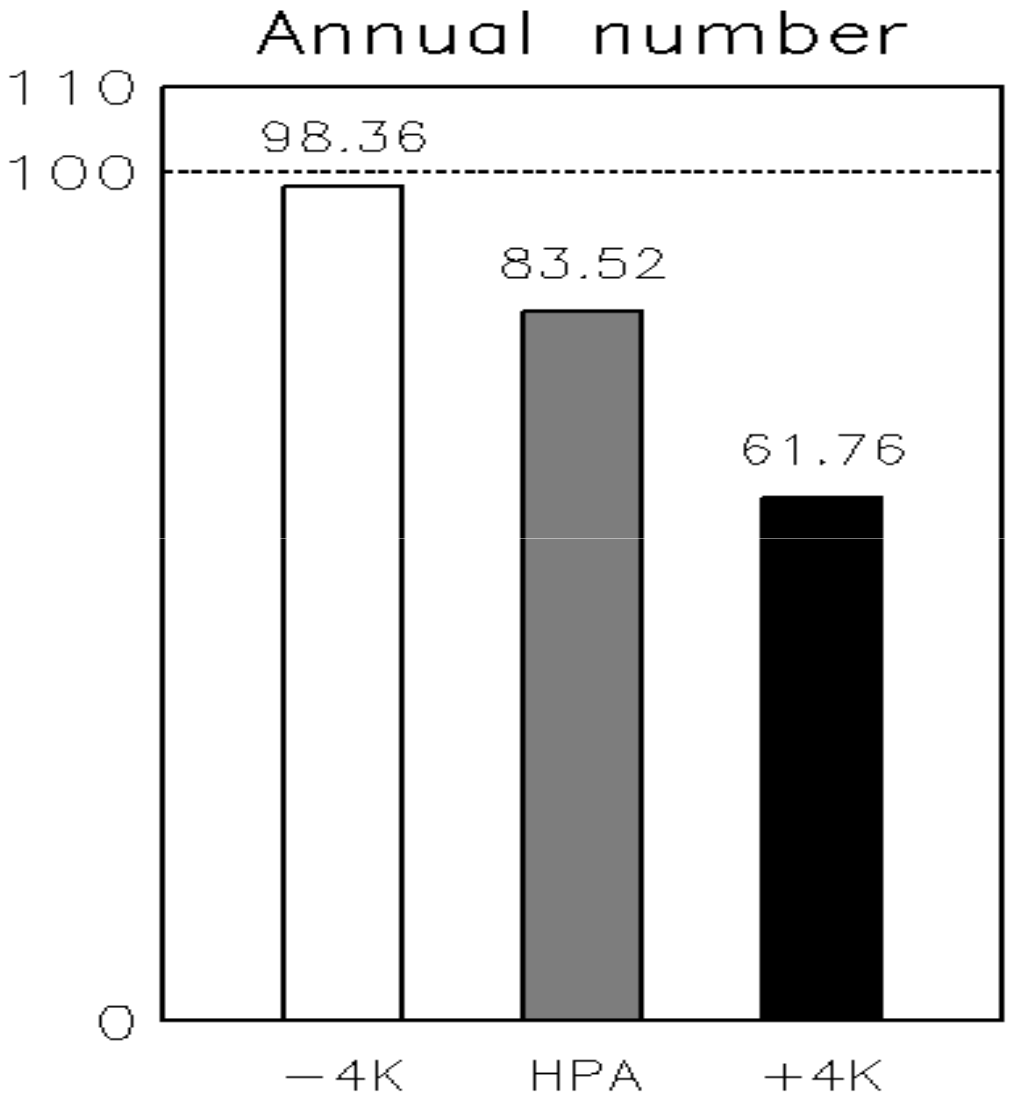

Criterion: Murakami et al. (2012)

MAX VORT : 8.0×10^{-5} [/s]

ΔPS : 0.2 [hPa]

MAX $WIND_{850}$: 13.0 [m/s]

MAX $WIND_{850}$ > MAX $WIND_{300}$: ON

WARMCORE ΔT: 0.8[K]

台風の数と安定度、降水量、上昇流の変化

	4K寒冷化	現在	4K温暖化
S: 安定度(K)	37.0	44.1	53.3
P: 降水量(mm/day)	3.07	3.50	4.00
ω: 上昇流(hPa/hr)	1.81	1.61	1.45
N: 年平均台風数	98.4	83.5	61.8

$$\frac{\Delta\omega}{\omega} \approx \frac{\Delta P}{P} - \frac{\Delta S}{S}$$

温暖化すると、降水量は増えるが、それ以上に安定度が増え上昇流は弱くなる。

寒冷化すると、降水量は減るが、それ以上に安定度が減り上昇流は強くなる。

季節ごとの台風発生場所と海面水温分布

7月－9月

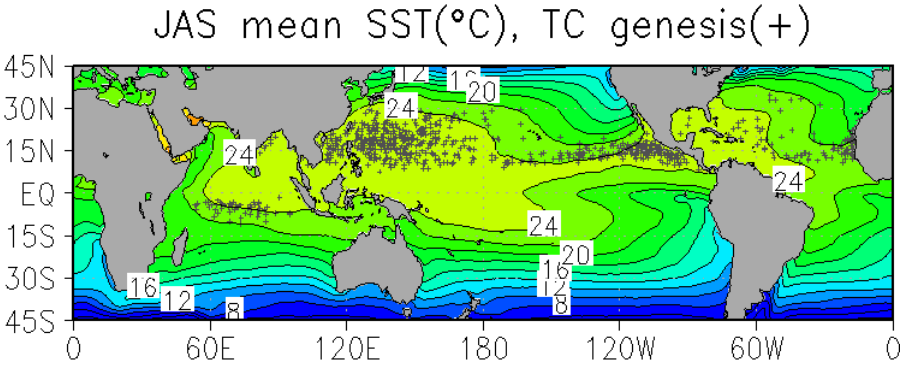

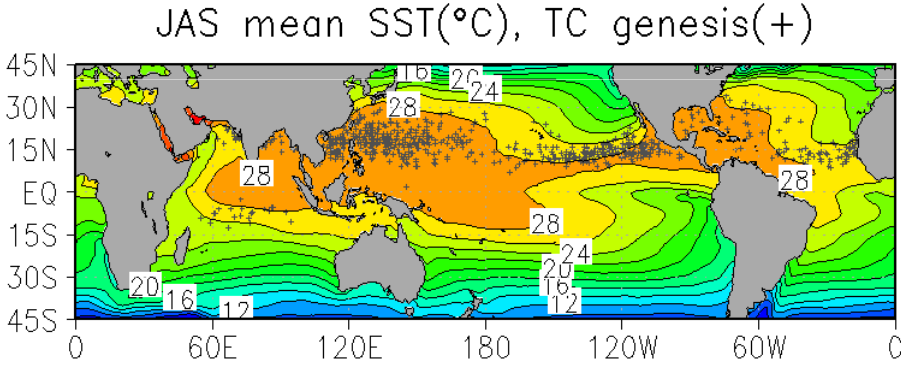

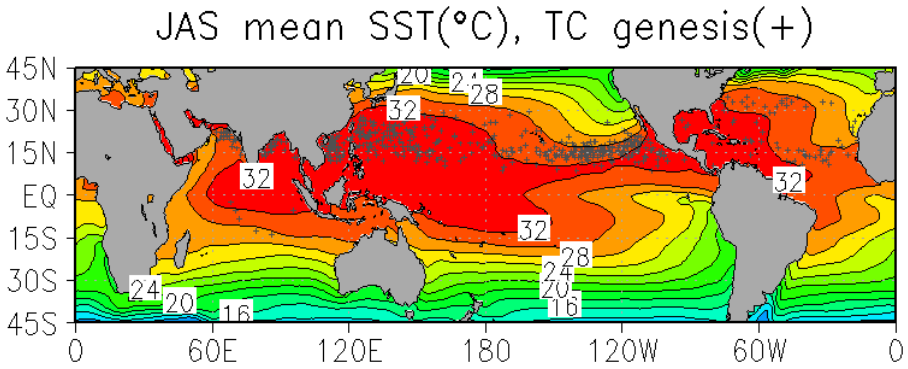

1月－3月

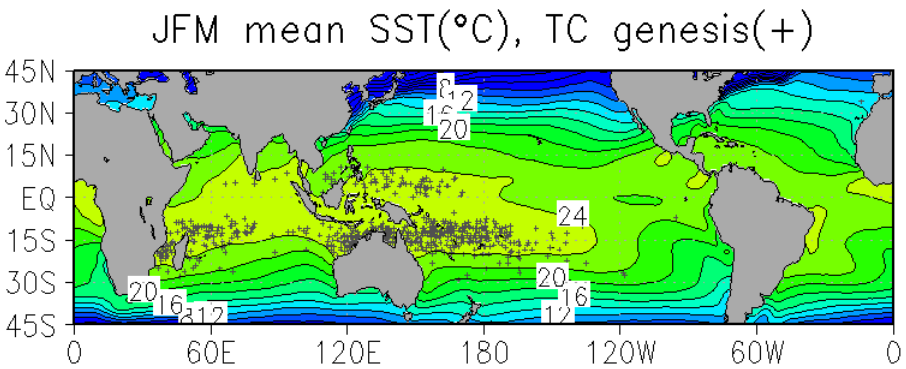

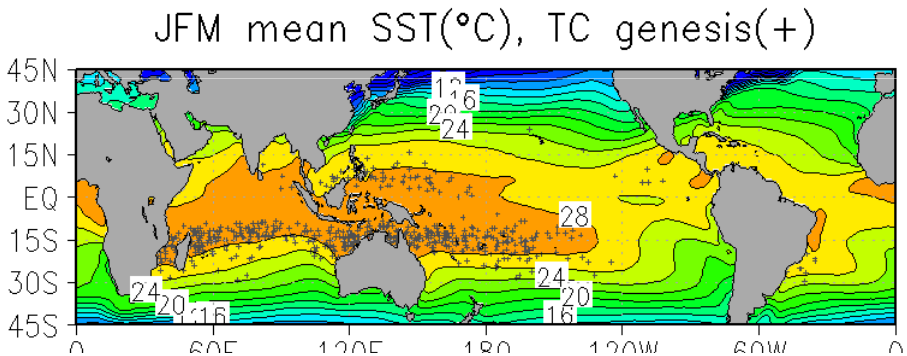

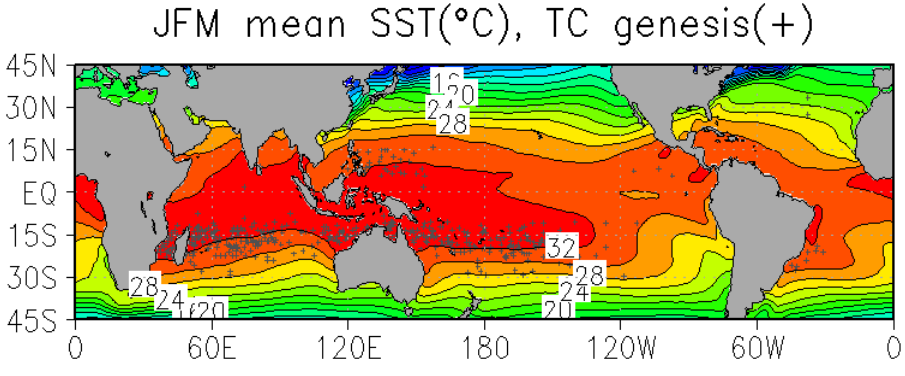

台風発生時の海面水温(全球)

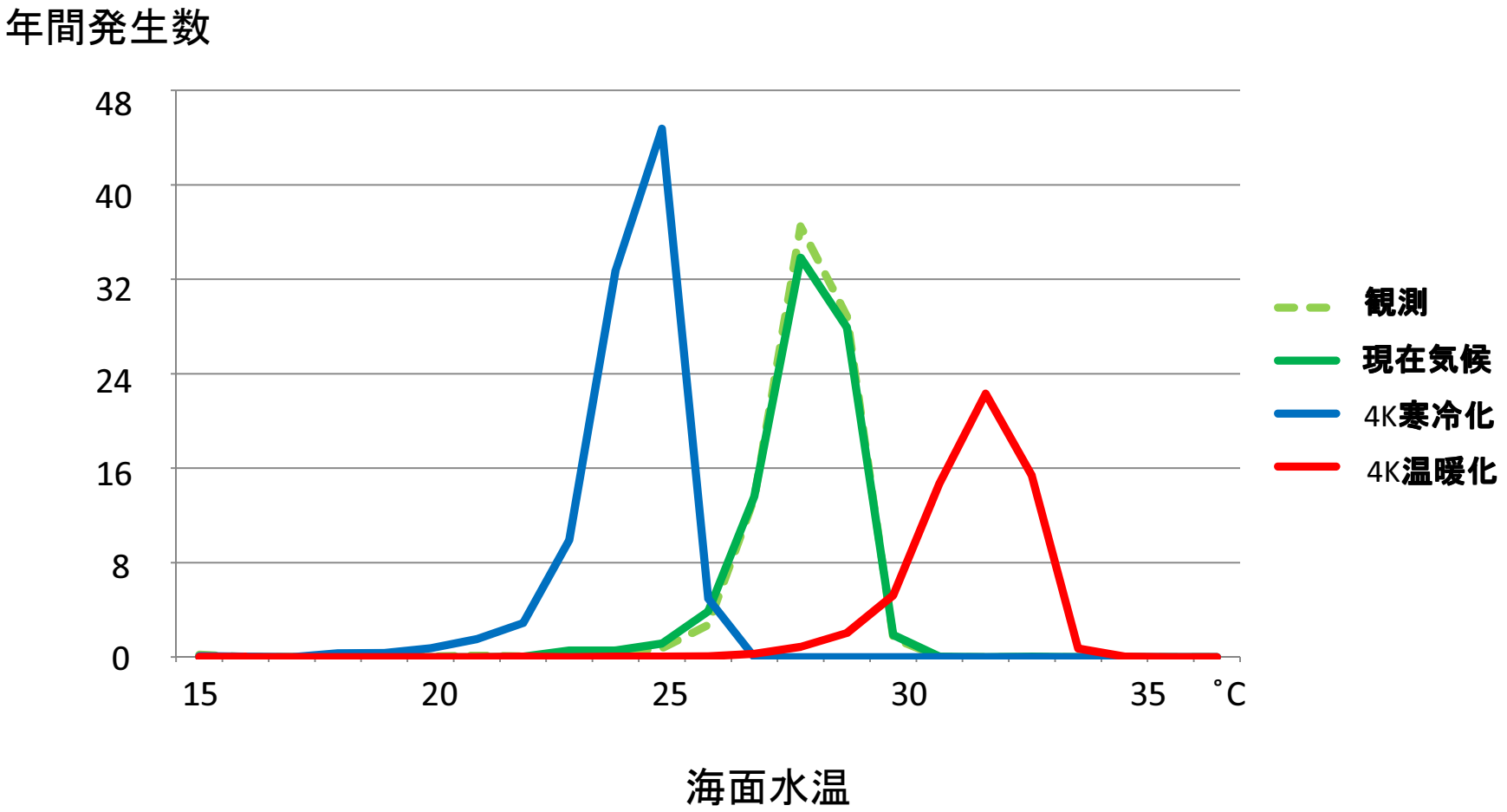

まとめと考察

◆ 4K寒冷化実験により、地球が寒冷化すると、降水量は減るが、それ以上に安定度が減り、上昇流（マスフラックス）が強くなり、全球の台風の数が増加することが示された。

◆ 台風は海面水温が26.5℃より低い所でも発生することも示された。

◆ さらに寒冷化したら台風の数はもっと増えるだろうか？
海面水温が10℃以下でも台風は発生するだろうか？
氷河期には台風の数が多かっただろうか？

◆ 放射対流平衡の観点からは、地球が寒冷化しても対流は起きるので、対流が組織化してできる台風も発生すると考えられる。

◆ 海面水温が10℃以下の極域でポーラーロウ（台風と似ている）が存在していることから、このような低温でも台風が発生する可能性は十分あると考えられる。

II. 台風の発生・発達のメカニズム

1. Warm Core の発達 ← net heating
   凝結熱ー断熱冷却

2. 渦の発達 ← 下層収束、effective bulk entrainment
   2次循環が重要

3. 下層の水蒸気が重要

Kurihara (1975) JAS

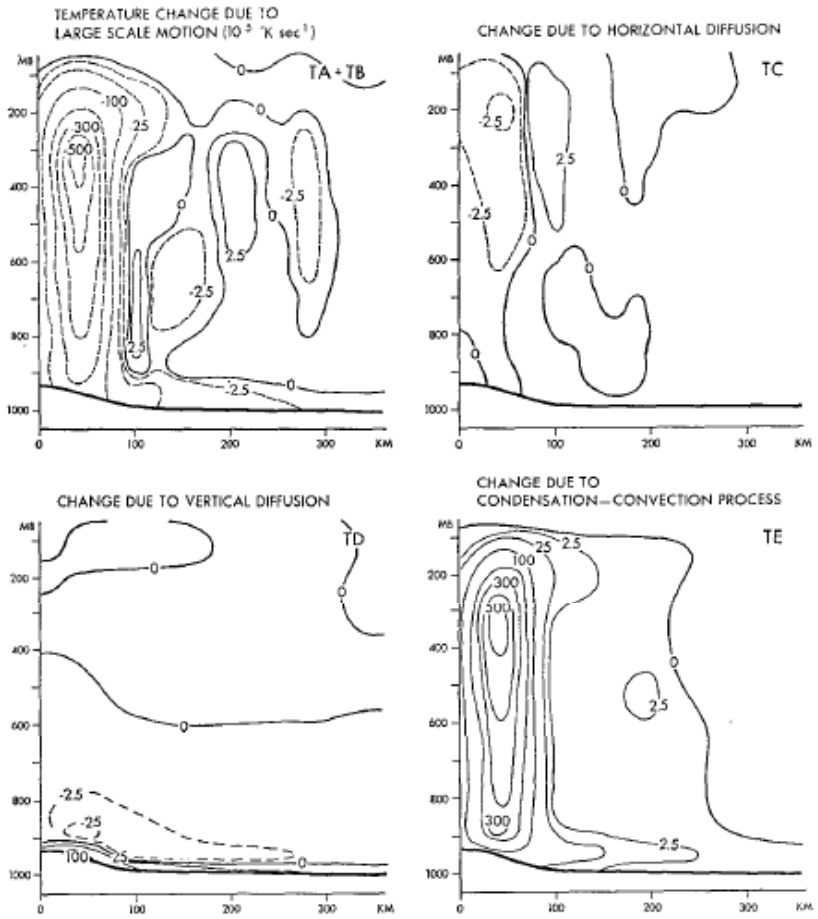

凝結熱 ≈ 断熱冷却

水蒸気多い ⇒ 同じマスフラックス
でも凝結熱大きい

net heating ≈ 凝結熱の数%

⇒ warm core の形成・発達

Ooyama (1969) JAS

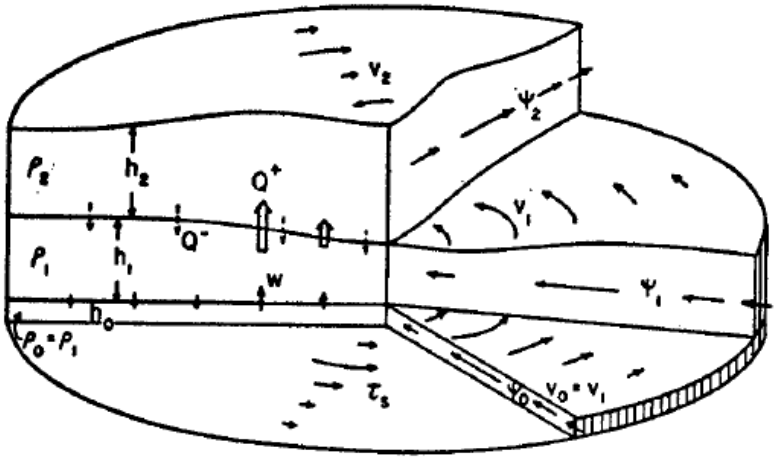

FIG. 1. Schematic diagram depicting the basic design of the model.

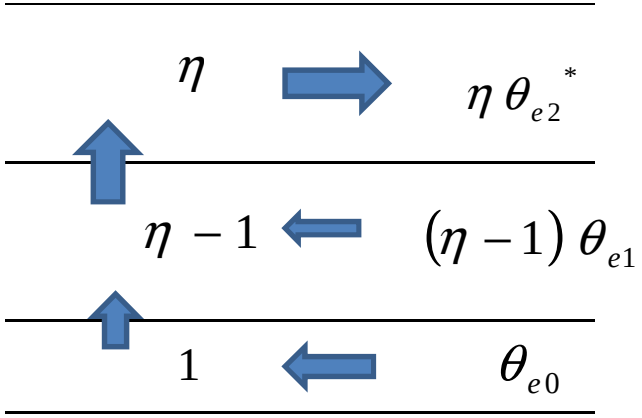

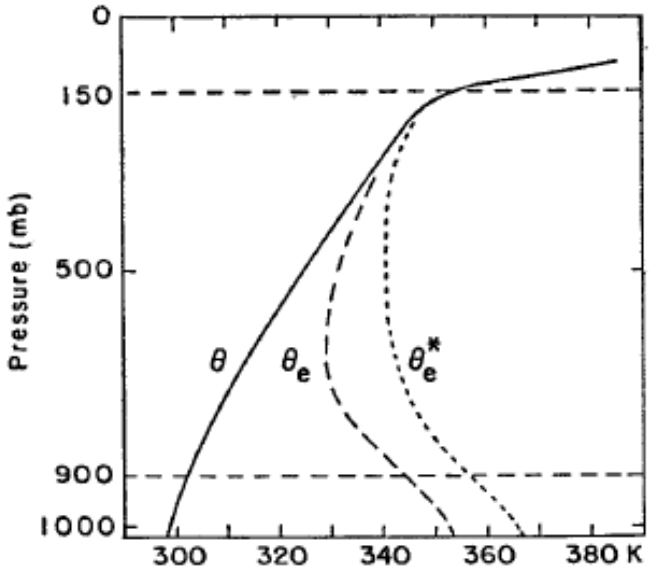

$$\eta = 1 + \frac{\theta_{e0} - \theta_{e2}^{*}}{\theta_{e2}^{*} - \theta_{e1}}$$

発達の条件:

$$\eta > 1 \quad (\theta_{e0} > \theta_{e2}^{*})$$

発達には条件付き不安定と
下層自由大気のインフローが必要

Charney and Eliassen (1964) JAS

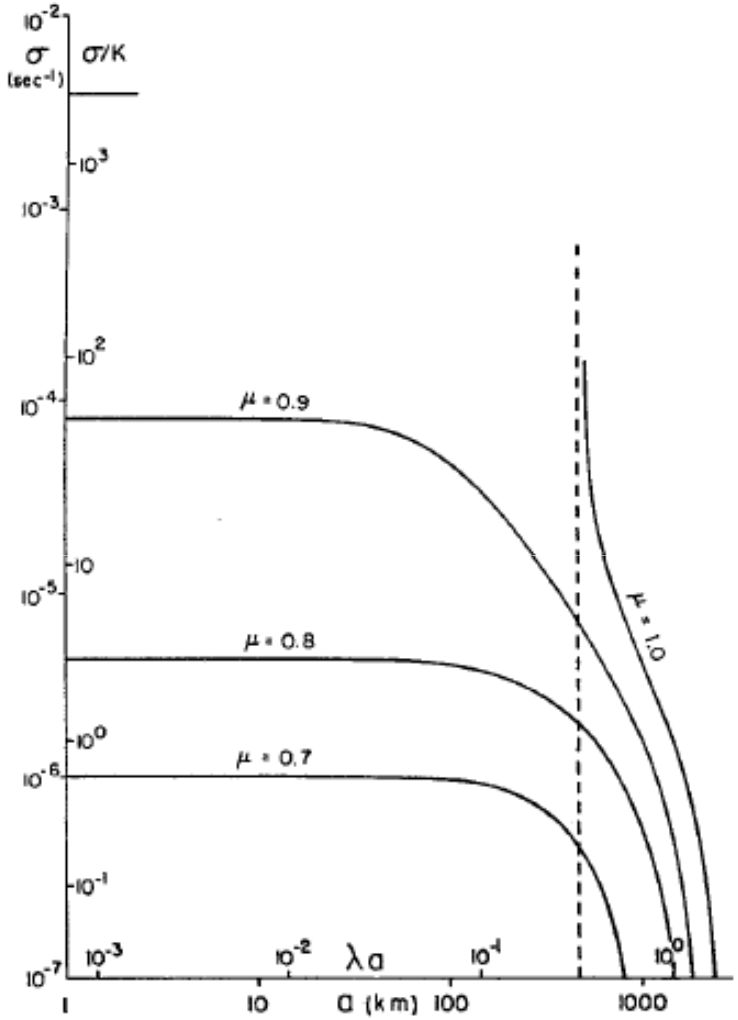

FIG. 1. The growth rate of the tropical depression as a function of the radius of the cloud region.

雲域（上昇域）半径： a
（ a ～100km ）

μ： 相対湿度
（上昇域のうち雲が占める割合）

μ＝0.7～0.8 の時に、
発達率 σ が 10日～1日
（台風スケールの発達率）

1次循環と2次循環のバランス

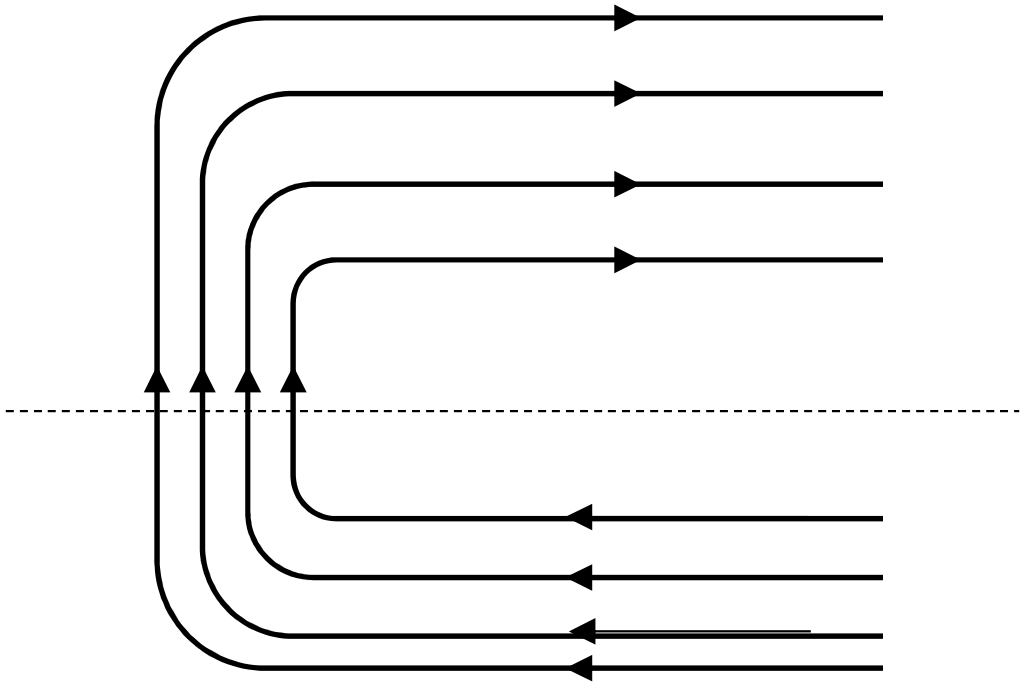

下層（境界層＋自由大気）で
収束した空気は、雲の中を上昇

実効バルクエントレインメント
下層大気の湿度が
net heating　をコントロール

Sawyer-Eliassen の方程式　：定常状態では上昇流とnet heating がバランス

$$\frac{\partial}{\partial r}\left(\frac{N^2}{r\rho_0}\frac{\partial \Psi}{\partial r}+\frac{-\overline{\xi}\,\overline{s}}{r\rho_0}\frac{\partial \Psi}{\partial z}\right)+\frac{\partial}{\partial z}\left(\frac{l^2}{r\rho_0}\frac{\partial \Psi}{\partial z}+\frac{-\overline{\xi}\,\overline{s}}{r\rho_0}\frac{\partial \Psi}{\partial r}\right)=-\frac{\partial \overline{\xi}\,\overline{F_v}}{\partial z}+\frac{g}{\theta_0}\frac{\partial \overline{Q}}{\partial r}$$

発達するためには、Q (net heating) が増加することが必要

What is the role of convection-scale vortices in the TC genesis?

20km-NHM

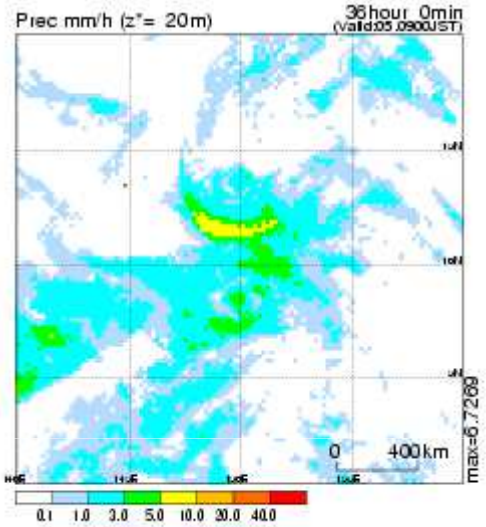

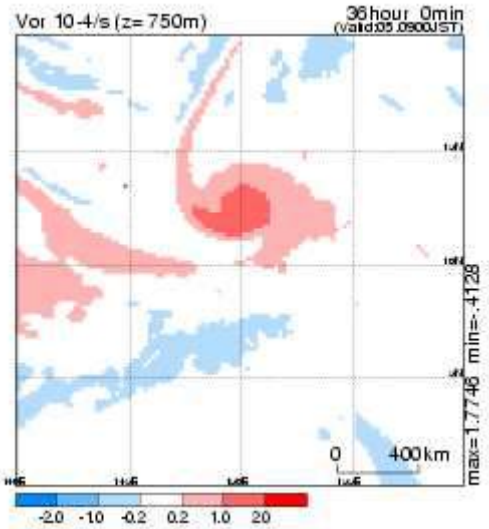

5km-NHM

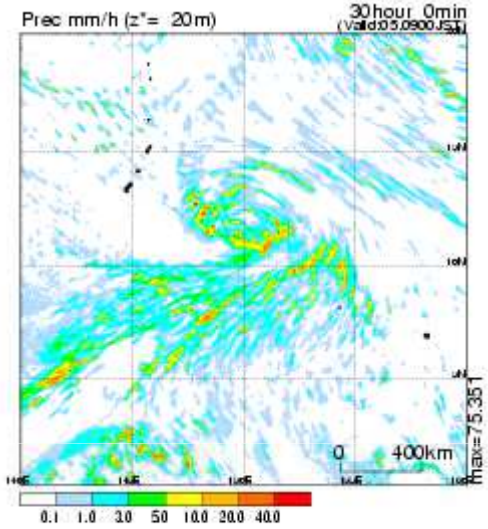

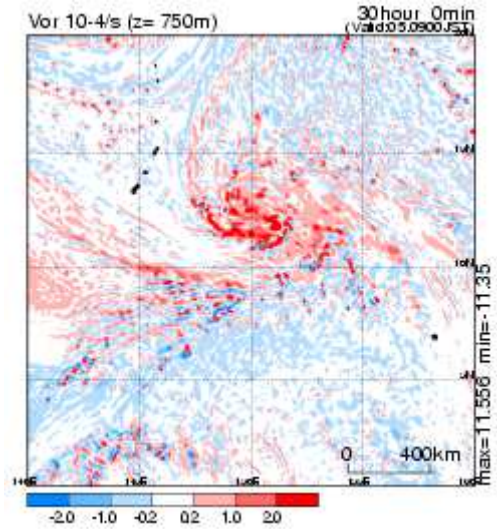

2km-NHM

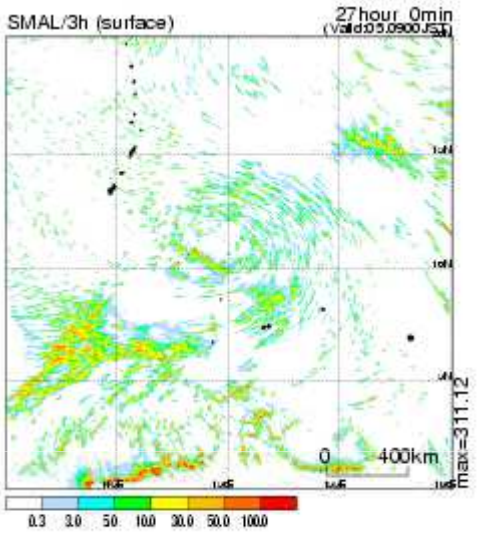

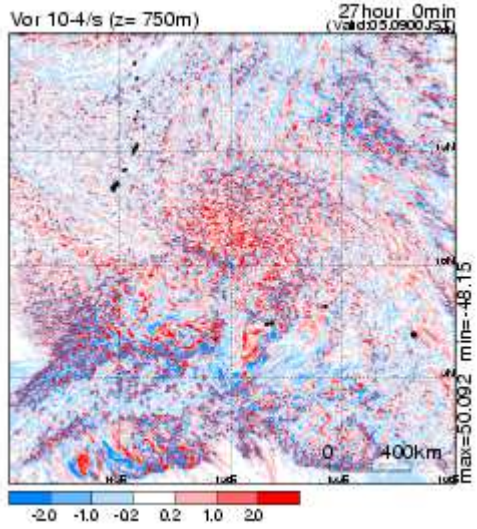

III. 最大可能強度（MPI）理論

Holland (1997)　JAS

Emanuel (1986)　JAS

Bister and Emanuel (2002)　JGR

地球が温暖化すると、なぜ台風全体の数が減るのに、強い台風の数が増えるのか

- ◆ 競争原理による格差の拡大説
- ◆ 最大強度増加説 （MPI理論）

温暖化すると台風の数は減る。しかし、強い台風は増える理由。

◆温暖化で、大気が安定化することで、熱帯擾乱全体に供給される運動エネルギーが減る。

◆しかし、一種の競争原理が働いて、少数の台風が限られエネルギーを独占し発達する一方で、多数の熱帯擾乱が台風の強さまで発達できなくなる。

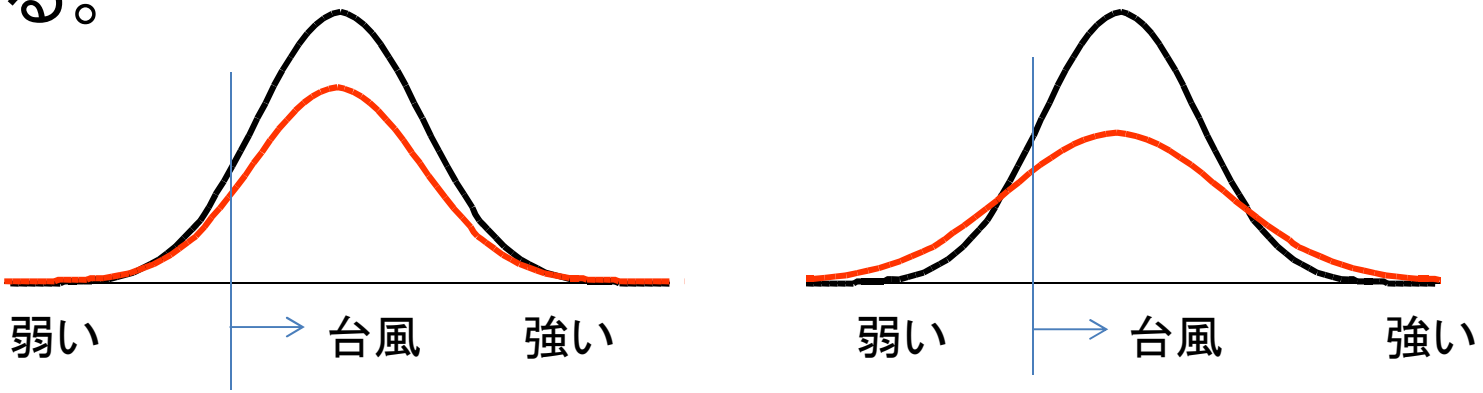

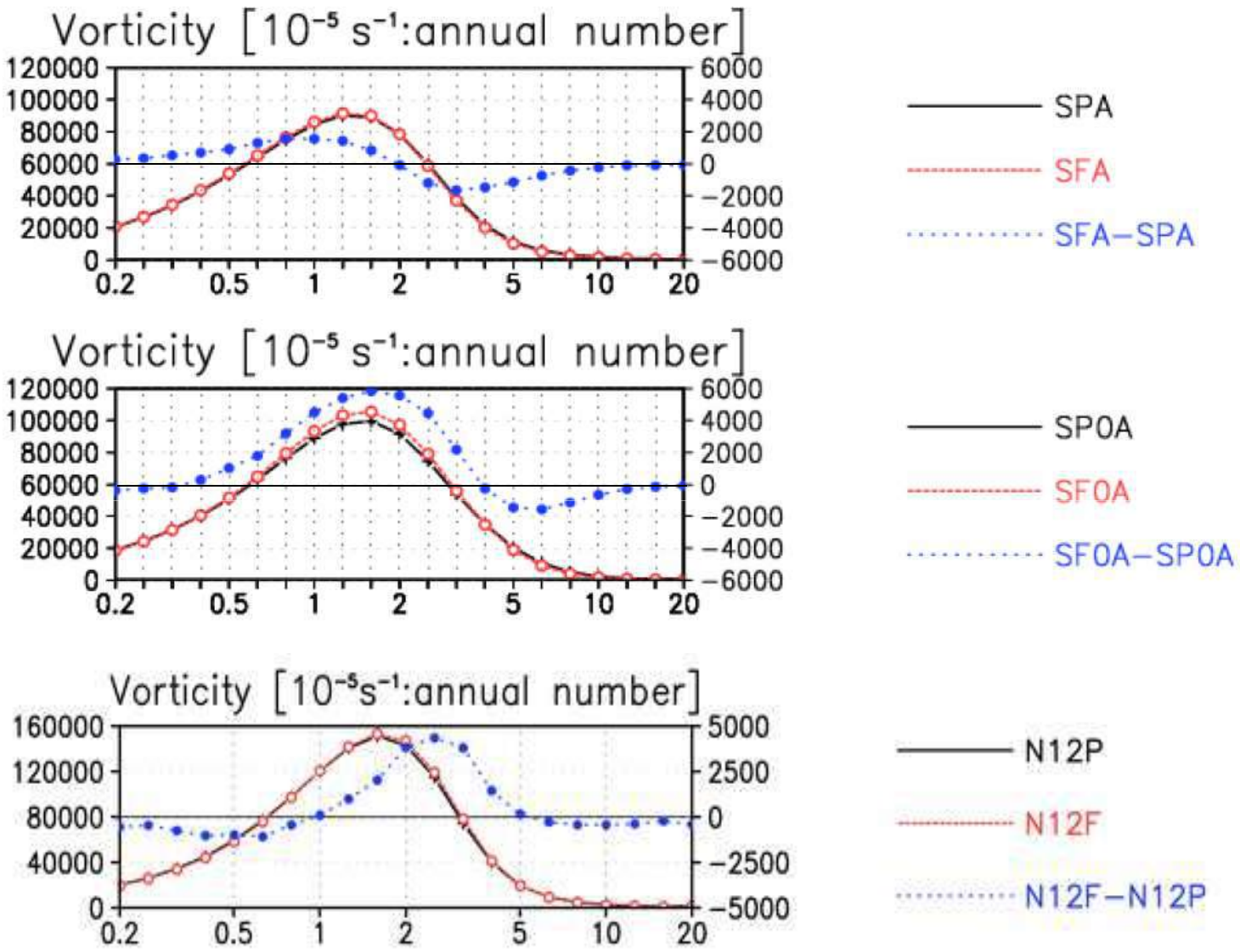

Yoshida 2013 and Yamada 2013

Holland のMPI

Holland (1997) JAS

Upright neutral　の仮定

$$\theta^*_{EC} = \theta_{ES}$$

$$\Delta T_{eyewall}(p) = \frac{\theta_{ES}\left(\frac{p}{1000}\right)^{\frac{R_d}{c_p}}}{\exp\left[1000\,q^*(1+0.81q^*)\left(\frac{3.376}{T}-0.00254\right)\right]} - T_{env}(p)$$

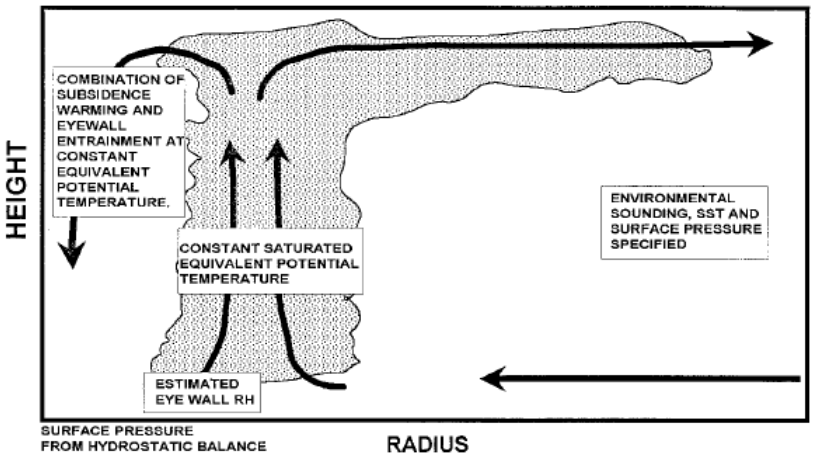

$$\Delta p_s = \frac{p_s}{T_v}\int_{p_s}^{p_T} \Delta T_v\, d\ln p$$

$$T_v = T(1+0.61q)$$

$$q_S = RHq^*_s \qquad q^*_S = \frac{\varepsilon\, e^*_s}{p_S}$$

p_s小 → q_s 大 → θ_{ES} 大 → ΔT 大

Emanuel のMPI (1)

Emanuel (1986) JAS

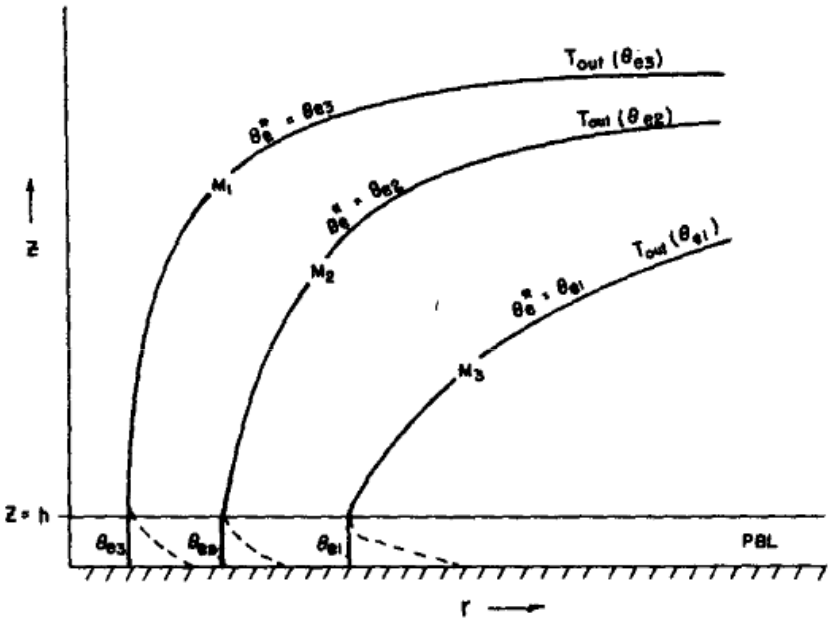

FIG. 1. Structure of the steady-state model. Curved lines above the planetary boundary layer (PBL) represent surfaces of constant angular momentum (M) and saturated equivalent potential temperature (θ_e^*). Solid lines in PBL show surfaces of constant θ_e while M is shown by dashed lines.

静力学バランス

$$\alpha \frac{\partial p}{\partial z} = -g$$

傾度風バランス

$$\alpha \frac{\partial p}{\partial r} = \frac{V^2}{r} + fV = \frac{M^2}{r^3} - \frac{1}{4} f^2 r$$

$$M = rV + \frac{1}{2} fr^2$$

傾斜中立 (Slantwise neutrality)

$\theta_e^* = \theta_{eB}$ along const. M surface

$$-r^2\frac{ds^*}{dM}(T_B-T_{out})=M \quad at \quad z=h \qquad (12)$$

θ_e と V の関係式

$$s^*=C_p\ln\theta_e \qquad \pi=\left(\frac{p}{p_0}\right)^{\frac{R}{C_p}}$$

p と V の関係式（傾度風の式）を用いると、θ_e と p の関係式が導かれる

$$-\frac{T_B-T_{out}}{T_B}\ln\frac{\theta_e}{\theta_{ea}}=\ln\left(\frac{\pi}{\pi_a}\right)+\frac{1}{2}r\frac{\partial\ln\pi}{\partial r}+\frac{1}{4}\frac{f^2}{C_pT_B}(r^2-r_0^2) \;\; at \;\; z=h \quad (18)$$

傾度風の式 $\frac{RT}{p}r\frac{\partial p}{\partial r}=V^2+frV$ 旋衡風の式 $\frac{1}{2}r\frac{\partial\pi}{\partial r}=\frac{1}{C_pT_B}\left(\frac{1}{2}V^2\right)$

(18) 式で、右辺最後の項を省略し、eyewall で旋衡風を仮定すると、

$$RT_B\ln\left(\frac{p_a}{p_m}\right)=C_p(T_B-T_{out})\ln\frac{\theta_{em}}{\theta_{ea}}+\frac{1}{2}V_m^2=(CAPE_m-CAPE_a)+\frac{1}{2}V_m^2 \quad (18')$$

Emanuel (1986) JAS

境界層のエネルギー（エントロピー）収支・角運動量収支から、

$$-\left.\frac{\partial s}{\partial M}\right|_{z=h} = -\left.\frac{\tau_s}{\tau_M}\right|_{z=0} = \frac{C_p C_\theta V(\ln\theta_{es} - \ln\theta_e)}{C_D r V^2} \quad (32), (33)$$

$$-\frac{ds^*}{dM} = \frac{M}{r^2(T_B - T_{out})} = \frac{V + \frac{1}{2}fr}{r(T_B - T_{out})} \quad (12)$$

$$\ln\theta_{es} - \ln\theta_e = \frac{C_D}{C_\theta}\frac{1}{C_p(T_B - T_0)}\left(V^2 + \frac{1}{2}frV\right) \quad (34)$$

Eyewall で旋衡風を仮定すると

$$V_m^2 = \frac{C_\theta}{C_D}C_p(T_B - T_0)(\ln\theta_{es} - \ln\theta_e) = \frac{C_\theta}{C_D}(CAPE_m^* - CAPE_m) \quad (34')$$

(18') 式と(34') 式から

$$RT_B \ln\left(\frac{p_a}{p_m}\right) = \frac{1}{2}V_m^2 + (CAPE_m - CAPE_a)$$

$$V_m^2 = \frac{C_\theta}{C_D}(CAPE_m^* - CAPE_m)$$

Bister and Emanuel (2002) JGR

境界層のエネルギー収支で、摩擦熱を考慮 (Bister and Emanuel 1998)

$$-\left.\frac{\partial s}{\partial M}\right|_{z=h} = \frac{C_p C_\theta V(\ln\theta_{es} - \ln\theta_e) + V^3/T_B}{C_D r V^2}$$

$$\ln\theta_{es} - \ln\theta_e = \frac{C_D}{C_\theta}\frac{1}{C_p(T_B - T_0)}V_m^2 - \frac{C_D}{C_\theta}\frac{1}{C_p T_B}V_m^2 = \frac{T_0}{T_B}\frac{C_D}{C_\theta}\frac{1}{C_p(T_B - T_0)}V_m^2$$

$$RT_B \ln\left(\frac{p_a}{p_m}\right) = \frac{1}{2}V_m^2 + (CAPE_m - CAPE_a)$$

$$V_m^2 = \frac{T_B}{T_0}\frac{C_\theta}{C_D}(CAPE_m^* - CAPE_m)$$

←Emanuel HP program

$$\frac{T_B}{T_0} \approx 1.5$$

Emanuel 1986とは50%も違う

$$C_p T_B \ln\left(\frac{p_a}{p_m}\right) = \frac{1}{2}V_m^2 + CAPE_m$$ ← Bister and Emanuel (2002) (4)式は 正しくない

台風カルノーサイクルアナロジー

Emanuel (1986) JAS

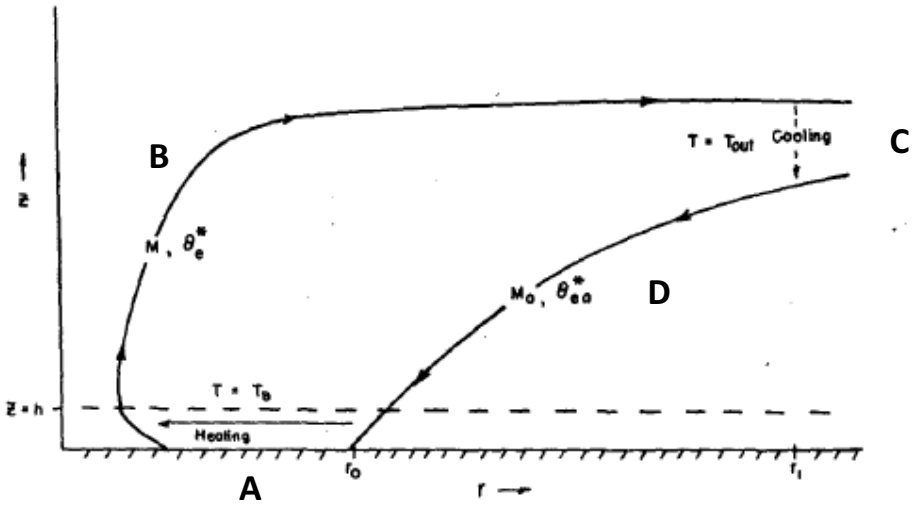

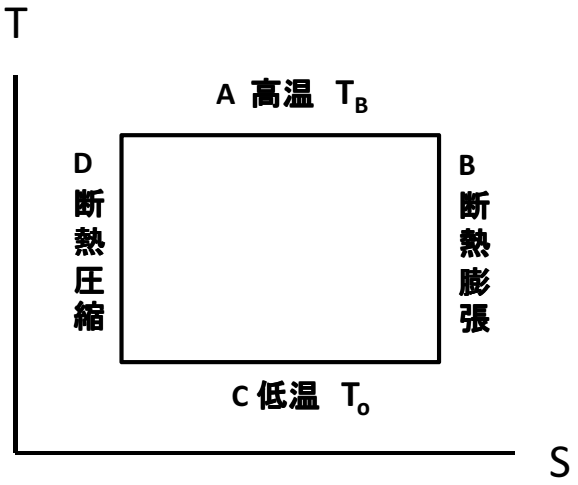

台風とカルノーサイクルの違い

B： 台風では潜熱の放出がある。浮力による加速（運動エネルギー生成）がある。
　　一方、外部への仕事は考慮されていない。

C： 台風では放射冷却は主にDで起きる。

D： 外部からされる仕事は、Bで外部に対してする仕事とキャンセル？

A： 定常状態の台風では、気圧傾度力による加速と摩擦による減速がバランス。
　　摩擦による加熱はカルノーサイクルにはない。

IV.　発生ポテンシャル（GPI）

Gray (1975)　CSU paper

Royer et al. (1998)　Clim. Change

Emanuel and Nolan (2004)　Hurricane Conf.

Emanuel (2013) PNAS

McGauley and Nolan (2011) JCLI

Camargo (2014)

GPI (Genesis Potential Index)

Yearly Genesis Parameter (Gray 1975)

$$SGP \equiv |f| \left(\zeta_r \frac{f}{|f|} + 5 \right) \left(\left| \frac{\delta V}{\delta P} \right| + 3 \right)^{-1} E \quad \left(\frac{\delta \theta_e}{\delta P} \right) Max \left(\frac{RH - 40}{30}, 1 \right)$$

$10^{-5}\,s^{-1}$	vorticity	shear	ocean thermal energy	stability	humidity
	950hPa $10^{-6}\,s^{-1}$	950hPa -200hPa		500hPa -surface	500hPa -700hPa

$$E = \int_0^{60} \rho_w c_w (T - 26) dz$$

$$YGP = SGP_{JFM} + SGP_{AMJ} + SGP_{JAS} + SGP_{OND}$$

Convective Genesis Parameter (Royer et al. 1998)

$$CSGP \equiv |f| \left(\zeta_r \frac{f}{|f|} + 5 \right) \left(\left| \frac{\delta V}{\delta P} \right| + 3 \right)^{-1} CP$$

$CP = k \times P_c$ Convectivre potential

P_c : Convective precipitation (mm/day)

$$CYGP = CSGP_{JFM} + CSGP_{AMJ} + CSGP_{JAS} + CSGP_{OND}$$

Genesis Potential Index (Emanuel and Nolan 2004)

$$GPI \equiv \left|10^5 \eta\right|^{3/2} \left(\frac{\mathrm{RH}}{50}\right)^3 \left(\frac{V_{pot}}{70}\right)^3 (1 + 0.1 V_{shear})^{-2}$$

vorticiy (s^{-1}) | humidity 700hPa | potential intensity (m/s) | shear (m/s) 850hPa - 250hPa

$$V_{pot}^2 = c_p (T_s - T_0) \frac{T_s}{T_0} \frac{C_k}{C_D} (\ln \theta_e^* - \ln \theta_e)\Big|_m$$

$$Y = X_1^{\,a} \cdot X_2^{\,b} \cdot X_3^{\,c} \cdot X_4^{\,d}$$

$$\ln Y = a \ln X_1 + b \ln X_2 + c \ln X_3 + d \ln X_4$$

$$\frac{\Delta Y}{Y} = a \frac{\Delta X_1}{X_1} + b \frac{\Delta X_2}{X_2} + c \frac{\Delta X_3}{X_3} + d \frac{\Delta X_3}{X_3}$$

Genesis Potential Index (Emanuel 2013)

$$GPI \equiv \left|\eta\right|^3 \chi^{-4/3} \, Max((V_{pot} - 35\mathrm{m}\cdot\mathrm{s}^{-1}), 0)^2 \, (25\mathrm{m}\cdot\mathrm{s}^{-1} + V_{shear})^{-4}$$

vorticity: 850hPa, $10^{-5}\,s^{-1}$ | humidity: 600hPa | potential intensity | shear: 850hPa - 250hPa

$$\chi = \frac{h^* - h_m}{h_0^* - h^*}$$

Saturation deficit : increase with temperature

$$V_{pot}^2 = c_p (T_s - T_0) \frac{T_s}{T_0} \frac{C_k}{C_D} (\ln \theta_e^* - \ln \theta_e)\Big|_m$$

$$\Lambda = \frac{V_{shear}\,\chi}{V_{pot}}$$

Ventilation Index
Tang and Emanuel (2012)

Potential intensity :
- increase with θ^*_e
- increase with SST (T_s) and
- decrease with outflow temperature (T_0)

T_s+2K: V_{pot}=45m/s → 64m/s
T_s+2K, T_0+3.4K: V_{pot}=45m/s → 61m/s

Genesis Frequency Index (GFI) McGauley and Nolan (2011) JCLI

$$GFI = f_{shear}\, f_{Vpot}\, f_{vorticity}\, f_{humidity}$$

f_X : frequency of finding X below (above) the threshold value

Poisson Regression Method Tippett et al. (2011) JCLI

$$P(N = n) = \frac{e^{-\mu}\mu^n}{n!}$$

N : 2.5˚ x 2.5˚ grid box の1か月の台風発生数
μ : 平均台風発生数

$$\mu = \exp(b + b_\eta \eta + b_H H + b_T T + b_V V + \log\cos\phi)$$

η : 850hPa absolute vorticity ($10^5 s^{-1}$), H : 600hPa relative humidity (%)
T : relative SST (˚C), V : vertical shear between 850hPa and 200hPa (ms^{-1})

今後の課題

変化のメカニズムの理解

台風の発生数の変化

- upward mass flux hypothesis
- saturation deficit hypothesis

⇒ upward mass flux またはsaturation deficit と台風の発生数の関係の理解が不十分

最大可能強度（MPI）理論

⇒ 改良の余地あり

発生ポテンシャル（GPI）

⇒ 統計式を気候変化に適用することの限界